DOE/PC/92541--T15

Exploring the Fundamentals of Radical Assisted NO_x Reduction Processes of Coal Combustors

Final Report
of
Grant DE-FG22-92PC92541

to

U. S. Department of Energy

by

Karen Chess
Shi-Chune Yao
Armistead G. Russell

Carnegie Mellon University
Department of Mechanical Engineering

May 31, 1996

DISCLAIMER

Abstract

This report describes experimental studies performed at Carnegie Mellon University to study the parameters that affect the performance of plasma-assisted ammonia radical injection for NO_x control from stationary combustion sources. First, the NO_x reduction potential of hot ammonia injection was studied to determine whether the use of the plasma for radical generation was key to the high NO_x reduction potential of the plasma deNO_x process. It was found that while some of the NO_x reduction in the plasma deNO_x demonstration experiments could be attributed to the enhanced thermal breakdown of NH_3 into NO_x reducing radicals, the effect of using the plasma accounted for 15-35% absolute additional NO_x reduction beyond any thermal benefit. This benefit of using the plasma increases with increased excess air and decreased flue gas temperature.

With the benefit of using the plasma verified on the larger scale of a demonstration experiment, two additional experiments were performed to study the parameters that affect plasma deNO_x performance on the local level. The opposed flow experiment failed to produce significant NO_x reduction, although it did highlight some key aspects of plasma performance with ammonia injection. Among these were the temperature drop with ammonia addition, and the ability of the plasma to produce NO_x with or without ammonia addition in an air environment. The production is easily precluded by depriving the plasma of oxygen. It was also found that the NO/NO_x analyzer may read non-NO_x species, and this effect was documented for future research. These effects were likely not seen in the demonstration experiments due to dilution by the combustion gas stream.

The reverse injection experiment successfully demonstrated the effects of NO-stream temperature, plasma power, and ammonia flow rate on plasma deNO_x performance. NO_x reduction improves with decreasing plasma power and with increasing ammonia flow rate and NO-stream temperature. However, the lower limit of the temperature window for plasma deNO_x is significantly below that for thermal deNO_x systems. In addition, it was suggested that the improved performance of the plasma deNO_x system with increased ammonia addition was due in

part to the drop in plasma temperature associated with NH_3 addition, and not just the use of more reagent.

Finally, a preliminary study of the chemical kinetics of the plasma deNO_x system was performed. This study highlighted the importance of effective plasma temperature and the residence time of the reagent at that temperature to efficient radical generation. This relationship would explain why the plasma deNO_x process works better at lower powers, given the approximate residence time of the ammonia passing through the plasma device. In addition, chemical kinetic modeling showed that potentially only a small relative radical concentration may be created by the plasma, but that these radicals react very quickly with NO. Additional NO_x reduction is achieved via the longer time scale dissociation of ammonia. At the end of the modeling chapter, a brief look at current plasma modeling capabilities is presented with suggested application to designing an optimized plasma deNO_x system.

Table of Contents

Chapter 1: Introduction

The control of nitrogen oxide (NO_x) emissions from many utility boilers is required under the acid rain provisions of the 1990 Clean Air Act Amendments. While these provisions specify reduced emission factors achievable with combustion modifications, additional emission reductions may be necessary to comply with Title I of the Act to control ground-level ozone in some areas.[1] In addition, NO_x emissions can contribute to many other environmental problems like the formation of particulate nitrates and acid aerosols and the eutrophication of marine coastal ecosystems.[2] To meet current and future NO_x emission reduction requirements, control technologies beyond combustion modifications will be required. Post-combustion, flue gas treatment controls like selective non-catalytic reduction (SNCR) and selective catalytic reduction (SCR) are representative of one class of technologies for enhanced NO_x reduction using reagent injection techniques.

SCR and SNCR both use chemical reactions with ammonia (NH_3) or other agents to reduce the amount of NO_x emitted into the atmosphere. SNCR processes, such as Thermal DeNO$_x$ ™,[3] inject cold NH_3 into combustion flue gases and rely on a narrow temperature window of 1100-1370 Kelvin[4] to dissociate the NH_3 for subsequent reduction reactions. At lower temperatures, the ammonia is not dissociated and "slips" through the system to be emitted out of the stack unchanged. At higher temperatures, the ammonia reacts preferentially with oxygen in the stack to form NO_x. Operating within the temperature window, SNCR generally achieves 40% to 60% NO_x reduction in commercial applications, and additional reduction is achieved by combining SNCR with other combustion modification NO_x control techniques. In contrast, SCR can achieve 80% to 90% NO_x reduction by introducing a catalyst grid into the ammonia injection process to aid dissociation.[5] However, the introduction of the catalyst can increase the expense of the reduction process considerably. In addition, SCR applications are also limited by a temperature window that is catalyst-specific.[6]

In an effort to lessen the dependence on a temperature window and to avoid the expense of a catalyst, a new approach using plasma technology was developed for NO_x reduction. Since a plasma is a gas in which a significant fraction of the molecules are ionized, NO_x reducing

Typical Operating Conditions

Q_1 = 0.0 lpm (no flow in all tests)
Q_2 = 1.5 lpm argon
Q_3 = 20 lpm argon +
0.8 lpm ammonia

Forward Power = 400 Watts
Frequency = 27.12 MHz

Atmospheric Pressure

Water cooling (through inductance coil) approx. 10 gal/min.

Plasma Torch Dimensions

Outer diameter of torch: 2 cm
ID of outer tube: 1.8 cm
OD of inner tube: 1.6 cm
OD of central tube: 0.5 cm

Overall length approx. 13 cm

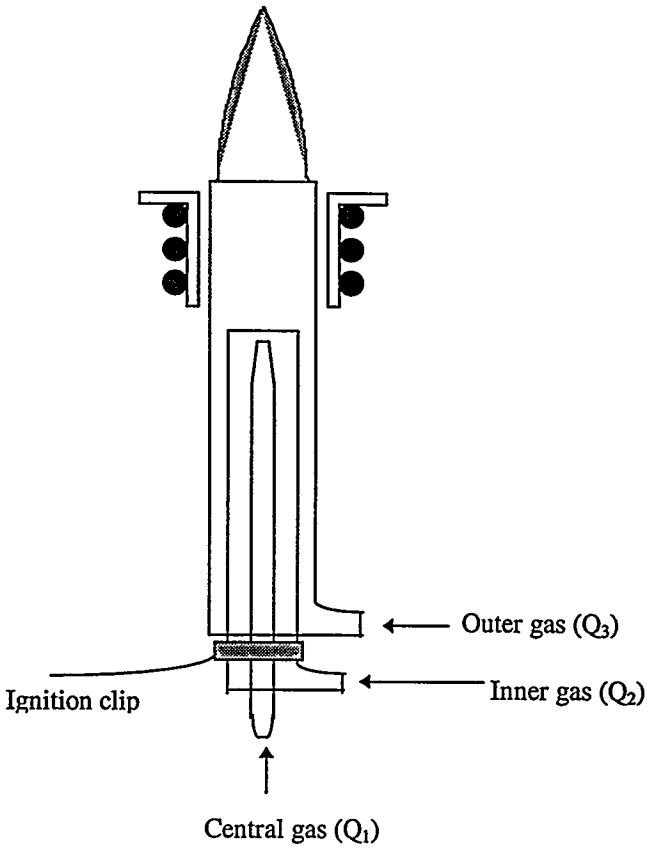

Figure 1.1: Inductively coupled plasma torch used by Zhou et al. in plasma deNO$_x$ demonstrations.

radicals may be effectively produced by allowing a reducing agent to interact with a plasma. In particular, ammonia radicals were created by passing the reagent through a plasma generator and then injected into combustion flue gases. By breaking down the NH_3 externally, the reliance on the temperature window and catalyst were avoided. Two independent studies of this "plasma deNO$_x$" process, one on a laboratory-scale combustor[7] and the other on a larger test facility,[8] demonstrated the potential of ammonia radical injection to achieve 80% to 90% NO$_x$ reduction.

At Carnegie Mellon University, Zhou used an inductively-coupled plasma (ICP) system originally designed for mass spectroscopy in her demonstration experiments.[9] A diagram of the plasma torch geometry is shown in Figure 1.1 along with typical system parameters. The induction coil creates an external time-varying magnetic field which interacts with charged particles flowing through the torch to form an electro-magnetically coupled system. Argon is used as the plasma gas because it is easy to strip it of an outer electron by a "Tesla" spark to initiate the plasma. In the NO$_x$ reduction experiments, ammonia was added after plasma ignition

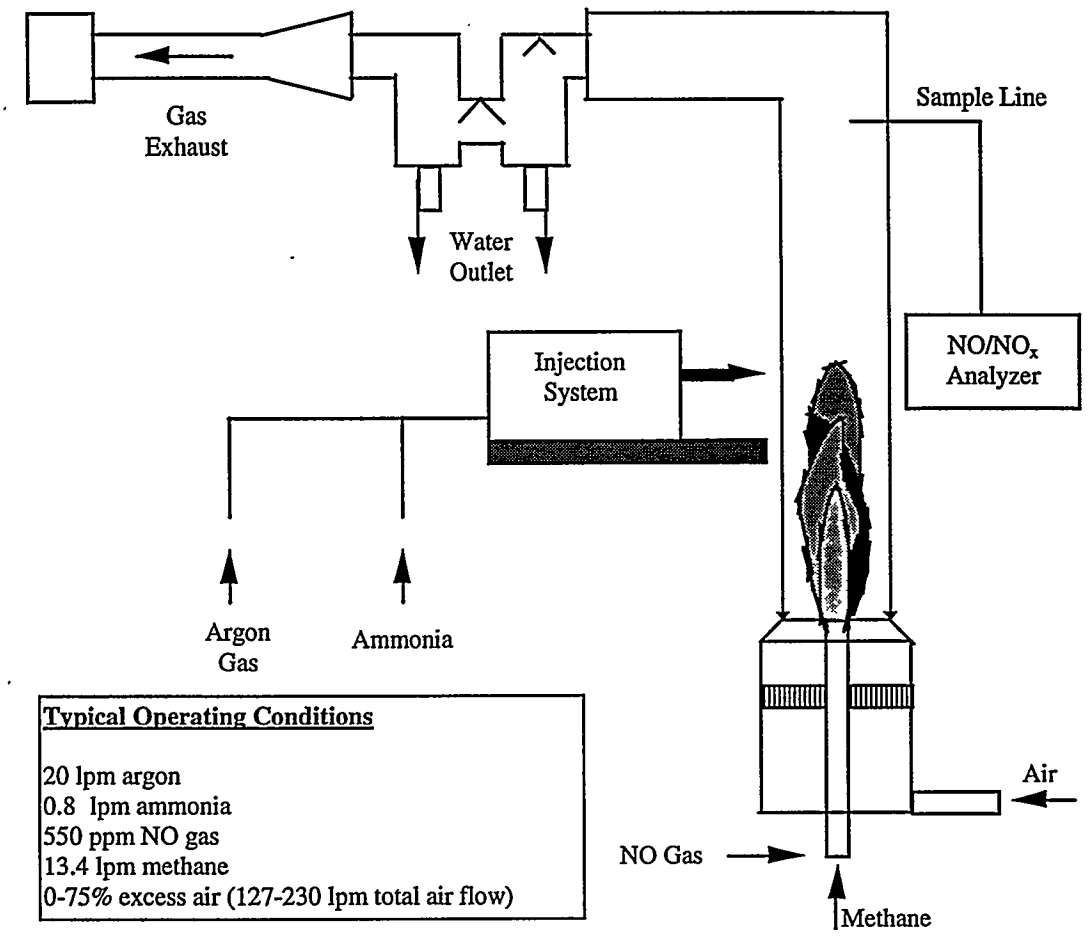

Figure 1.2: Carnegie Mellon University facility used by Zhou et al. for plasma deNO_x research.

to the outer argon gas stream (Q_3) with the goal of producing amidogen (NH_2) or other NO_x-reducing agents.

Figure 1.2 shows the overall apparatus used in Zhou's NO_x reduction experiments and lists typical operating conditions. The combustor and the fuel injector measured 15 cm and 1 cm in diameter, respectively, and the length of the combustion chamber was 150 cm. A methane diffusion flame was doped with nitric oxide to raise the NO concentration in the combustor to typical coal combustion conditions. NO and NO_x measurements were made downstream of the ammonia radical injection with a Thermo-Electron 10AR chemiluminescent NO/NO_x analyzer. Measurements were taken with and without ammonia addition through the plasma to determine NO_x reduction relative to a baseline value.

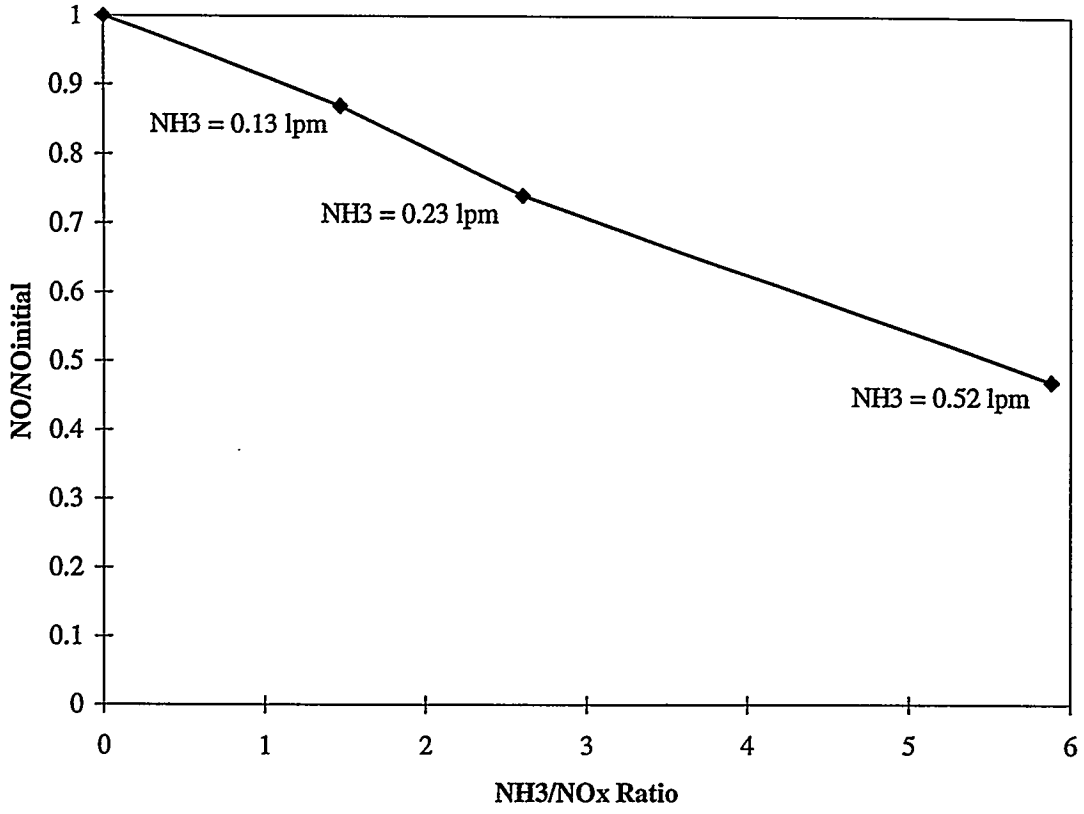

Figure 1.3: $NO/NO_{initial}$ vs. NH_3/NO_x ratio at 0% excess air in Zhou's demonstration experiments.

Zhou found a maximum NO_x reduction of 86%, and therefore demonstrated the feasibility of the plasma deNO_x process.[9] Also, this peak reduction occurred at a flue stream temperature of approximately 1000 K, which is below the temperature window required for SNCR. However, her data also suggested the need for additional experimentation to better understand the process. For example, Figure 1.3 shows NO_x reduction data from Zhou's experiments at 0% excess air combustion conditions for different NH_3/NO_x ratios. As shown, more ammonia led to better NO_x control; however, typical SNCR applications use an NH_3/NO_x ratio between 1 and 2, while Zhou found she needed ratios closer to 7 for optimum reduction. Thus, the parameters that affect the efficiency of ammonia use in the plasma system require further research. One of these parameters is likely to be plasma power, as shown in Figure 1.4. Lower power led to better NO_x reduction at 25% excess air in Zhou's demonstration experiments.

Since Zhou's experiments were for demonstration purposes, her work includes only limited data investigating the range of different parameters that affect plasma deNO_x performance. In addition, because the ammonia radicals in the plasma deNO_x process are necessarily injected at elevated temperatures, it must be considered that the high levels of NO_x reduction at peak performance could still be the result of increased NH_3 dissociation by thermal

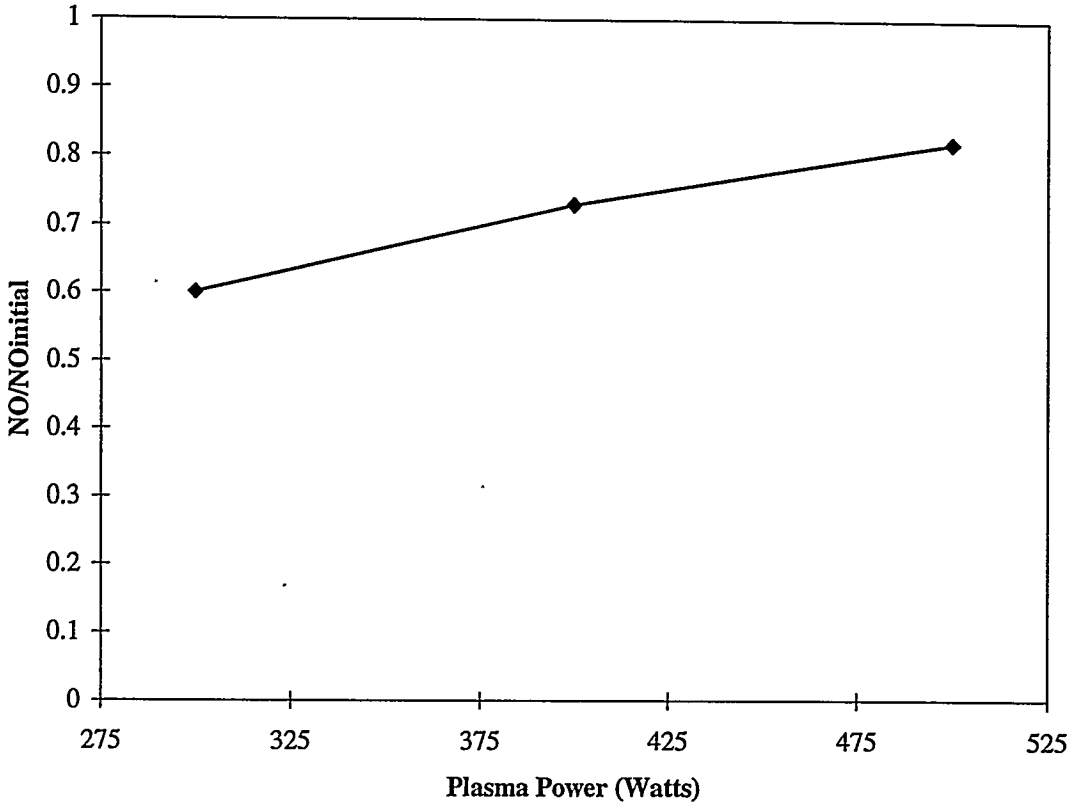

Figure 1.4: $NO/NO_{initial}$ vs. plasma power at 25% excess air conditions in Zhou's experiments.

breakdown, as well as the result of the presence of externally produced radicals. The goals of the current research are thus to

1. demonstrate that the benefit of the use of plasma technology in ammonia injection processes is beyond the benefit of bulk heating of the reagent.
2. examine the plasma $deNO_x$ process on a local level to explore the effects of plasma power and NH_3 flow rate on process efficiency.
3. investigate specifically the flue stream temperature limit of the plasma $deNO_x$ process.
4. consider possible modeling studies to explain observed trends.

Chapter 2 will present the results of an experiment on the performance of hot ammonia injection. This experiment was designed to mimic conditions in Zhou's plasma demonstration experiments, but with the substitution of hot NH_3 and argon carrier gas for the plasma injection system. By comparing the results to the demonstration experiments, it is shown that the benefit

of the interaction between the ammonia and the plasma is beyond the benefit of bulk heating of the ammonia for NO_x reduction. Chapters 3 and 4 then present results of experiments designed to investigate the parameters affecting the plasma deNO_x performance. Chapter 3 discusses an opposed flow experiment in which the interface of two jets, one NO_x-laden and the other formed by the NH_3-doped plasma, was studied. This experiment did not produce good NO_x-reduction results, although it did illustrate several performance characteristics of the plasma system. To better study the parameters affecting NO_x reduction by plasma deNO_x, the opposed flow experiment was replaced with a reverse injection set-up. In this experiment, described in Chapter 4, a NO_x stream was injected toward the plasma at close range. This set-up successfully allowed the exploration of the effects of ammonia flow rate, plasma power, and NO_x stream temperature on plasma deNO_x performance.

Following the reports on experimental activities, the results of chemical kinetic modeling to qualitatively explain the trends shown in the reverse injection experiment will be presented in Chapter 5. This chapter also includes a summary of current plasma modeling techniques and their potential application to study of the plasma deNO_x system. Chapter 6 will summarize the results in this report and will present recommendations for plasma deNO_x design and areas for future research.

Chapter 2: Hot NH_3 Injection for NO_x Control

Introduction

In the plasma deNO_x process for NO_x control, ammonia is passed through a plasma source to dissociate it into effective NO_x-reducing radicals. In the majority of Zhou's demonstration experiments, the power supplied to the ICP source was 400 Watts. While only a portion of this power is transferred to the plasma gases (the remainder being lost through the cooling system, EMF losses, and others), the fact that power is supplied to the ammonia before injection raises an important question. Since the radicals in the plasma deNO_x process are necessarily injected at elevated temperatures, the high level of NO_x reduction achieved could be the result of increased NH_3 dissociation by thermal breakdown within the combustor, as well as the result of the presence of externally produced radicals. These two effects, bulk thermal heating and radical production via interaction with the plasma, must be separated in order to determine if the application of plasma technology to NO_x control is the means by which the high NO_x reduction was achieved in the demonstration experiments.

To separate the thermal effect from the plasma effect, an experiment in hot ammonia injection for NO_x control was performed. In it, the lab-scale apparatus used in previous demonstrations of the process was modified by replacing the plasma system for ammonia radical injection with a system to inject hot NH_3 and a carrier gas. In this way, NO_x reduction by the thermal effect was allowed, but NO_x reduction by the plasma effect was prevented. The relative NO_x reduction of hot NH_3 to cold NH_3 injection, a measure of the thermal effect, was investigated directly. The advantage of the plasma injection over hot NH_3, a measure of the plasma effect, was inferred by duplicating conditions from the previous demonstration work, using hot injection instead of the plasma system. Thus, the hot injection experiment not only provides evidence concerning the mechanism of plasma deNO_x performance, but also served to investigate whether typical SNCR processes could be improved simply by heating the ammonia prior to injection.

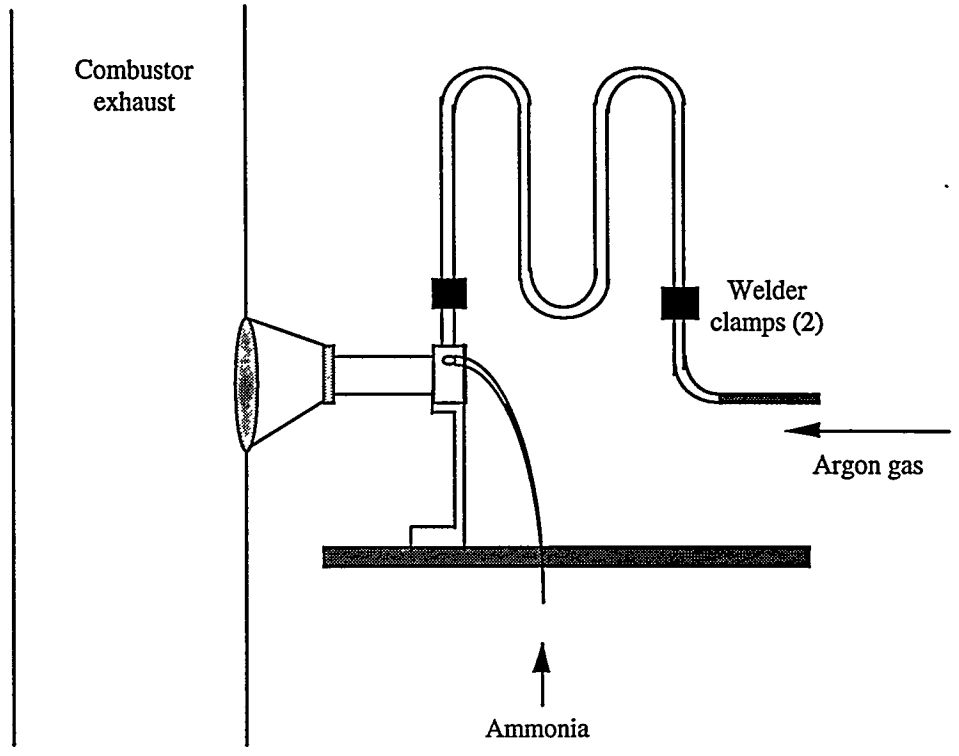

Figure 2.1: Hot ammonia injection apparatus replacing plasma system.

Experiment Design

Figure 1.2 showed the overall combustor system used in previous demonstration experiments by Zhou et al., and this same set-up was used for the hot injection investigations. The ammonia, carrier gas (argon), and combustion gas flow rates used in the plasma and hot injection experiments were identical. As described in Chapter 1, NO and NO_x concentration measurements were made with a Thermo-Electron Model 10AR chemiluminescent NO/NO_x analyzer. Gas flow measurements were made with rotameters, and temperatures were measured with Chromel-Alumel (Type K) thermocouples.

The plasma system used in the radical injection process was described briefly in Chapter 1. In the hot injection study, this system was replaced with an apparatus for heating and injecting hot ammonia carried on argon into the combustor, as shown in Figure 2.1. Argon was passed through a 100 cm stainless steel tube whose temperature was controlled by varying the DC current supplied to the tube for direct Joule heating. The hot argon gas the passed into an injector

designed to mimic the geometry (and therefore the swirling flow conditions) of the plasma torch. Cold NH_3 was introduced tangentially into the injector, where it mixed with the hot argon gas before being injected into the combustor. The injector was positioned approximately 8 cm from the combustor, as was the plasma torch in the previous experiments. An electrically insulated nozzle connecting the injector to the combustor minimized the amount of ambient air entrained by the hot jet. In the plasma experiments, a larger guard box produced a similar effect. Finally, the entire hot tube and injector were insulated to minimize heat loss.

The achievable temperatures of the gas exiting the hot tube apparatus were dictated by the limitations of the materials used. At peak operating conditions, the hot tube reached 1150 K with 740 W supplied by the electrical source. Only a portion of this power was actually used to heat the injected gases, with the remainder being lost thermally and radiatively. It is of concern whether the power input to the injection gases in the hot tube experiments was similar to the power input to the injection gases in the plasma experiments. In the subset of data selected from the plasma experiments for comparison, the power supplied to the plasma gun was 400 W, but only a portion is transferred to the plasma gases. At peak power in the hot tube experiments, the argon/ammonia stream entered the combustor at about 850 K. Based on this temperature and a mean specific heat and density of argon, the power actually carried into the combustor by the input gases was about 215 W. In the plasma experiments, the temperature at the injection section was reported as 920 K,[9] which would correspond to a power input of about 240 W. Thus, the power supplied to the injected gases in both experiments was comparable.

Results

Throughout the experiments, little or no difference was detected between the NO and NO_x measurements, which is consistent with commercial measurements indicating that 90% or more of NO_x emissions from utility boilers is NO. Since the combustion gases in the present experiments were doped with NO, emission reductions are reported as the percent NO reduction relative to a baseline of no ammonia injection. In reporting NO reduction performance at various temperature conditions, the following nomenclature is adopted. "Injection inlet temperature" is the temperature of the hot ammonia stream as measured along the centerline of the injection stream at a distance 1 cm before entering the combustor. "Flue gas temperature" is the

temperature of the combustion flue gas at the centerline of the combustor, as measured approximately 5 cm below the ammonia injection port.

Figure 2.2 shows the effect of injection inlet temperature on NO reduction for combustion at 25% excess air. As shown, NO reduction increases modestly as the temperature of the injected ammonia/argon stream is raised. The temperature in the combustor near the injection point for this set of data was about 975 K, below the temperature window that favors the dissociation of NH_3. Thus, the reduction values shown in the figure (25-40%) should seem high. However, a typical NH_3/NO_x ratio for the SNCR process is between 1 and 2,[10] while the ratio used to generate Figure 2.2 was roughly 7, corresponding to ratios typical of the lab-scale plasma experiments that led to high NO_x reduction for these combustion conditions. At higher concentrations of ammonia, more NO reduction would be expected.

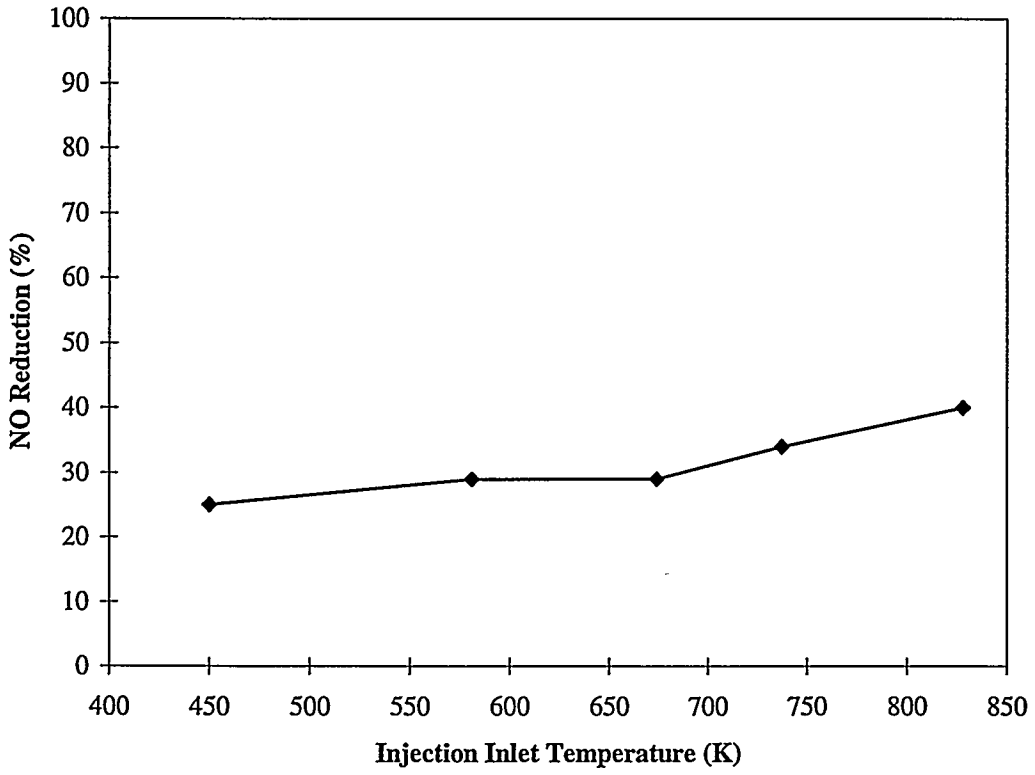

Figure 2.2: Effect of injection temperature on NO reduction at 25% excess air conditions.

To compare the NO reduction performance of the lab-scale apparatus at SNCR-favorable temperatures and commercial NH_3/NO_x ratios, the combustion flue gas temperature was raised to

over 1100 K and the ammonia flow rate was cut. Figure 2.3 shows the NO reduction achieved under 25% excess air conditions with cold and hot NH_3 injection for NH_3/NO_x ratios between 0 and 5. For ratios between 1 and 2, NO reduction values were typical for SNCR-like processes and, as expected, NO reduction increased with the addition of ammonia. Also, hot NH_3 injection led to slightly higher NO reduction values than cold injection at the same combustion and ammonia flow conditions over the range tested. Since the repeatability of the NO reduction data is ±5%, the advantage of hot injection at low NH_3/NO_x ratios is by no means proven. However, throughout the experiments, hot injection performed better than cold injection at the same conditions.

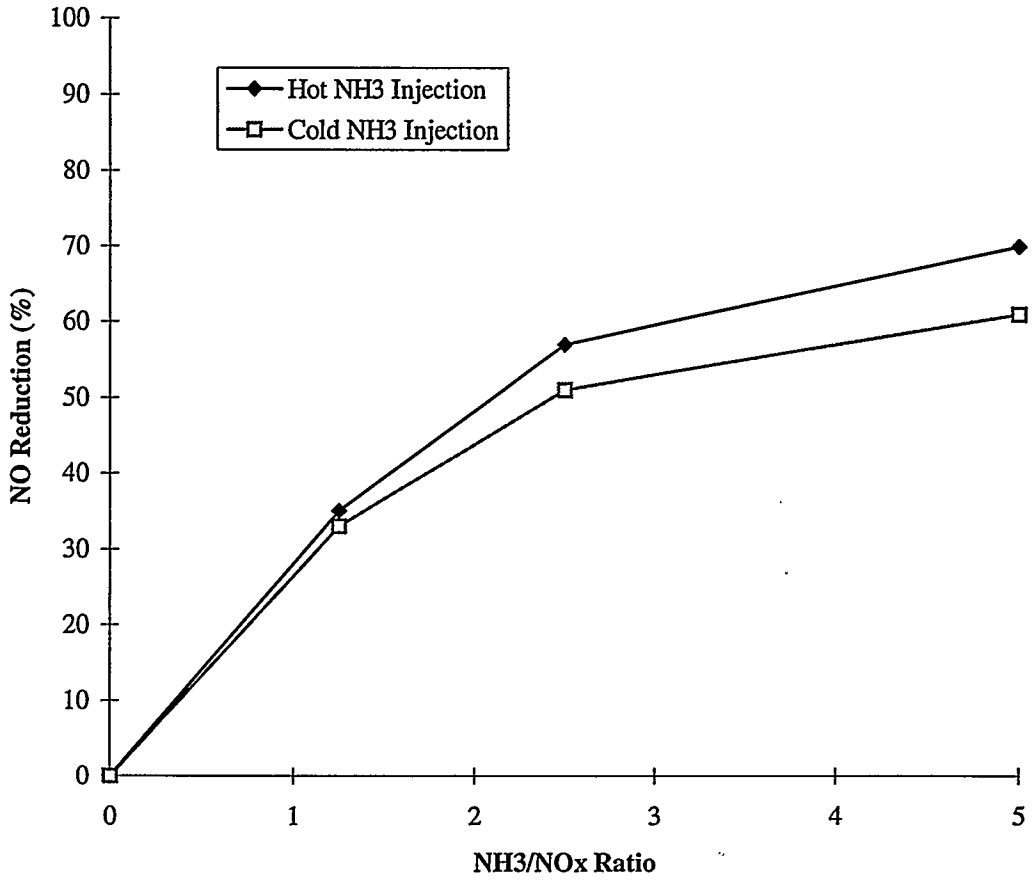

Figure 2.3: Effect of NH_3/NO_x ratio on NO reduction with cold and hot injection at 25% excess air.

Figure 2.4 shows typical results for NO reduction with cold and hot NH_3 injection over a range of combustor temperatures at 25% excess air conditions similar to those in the high reduction plasma experiments. As shown, hot NH_3 injection was moderately more effective than

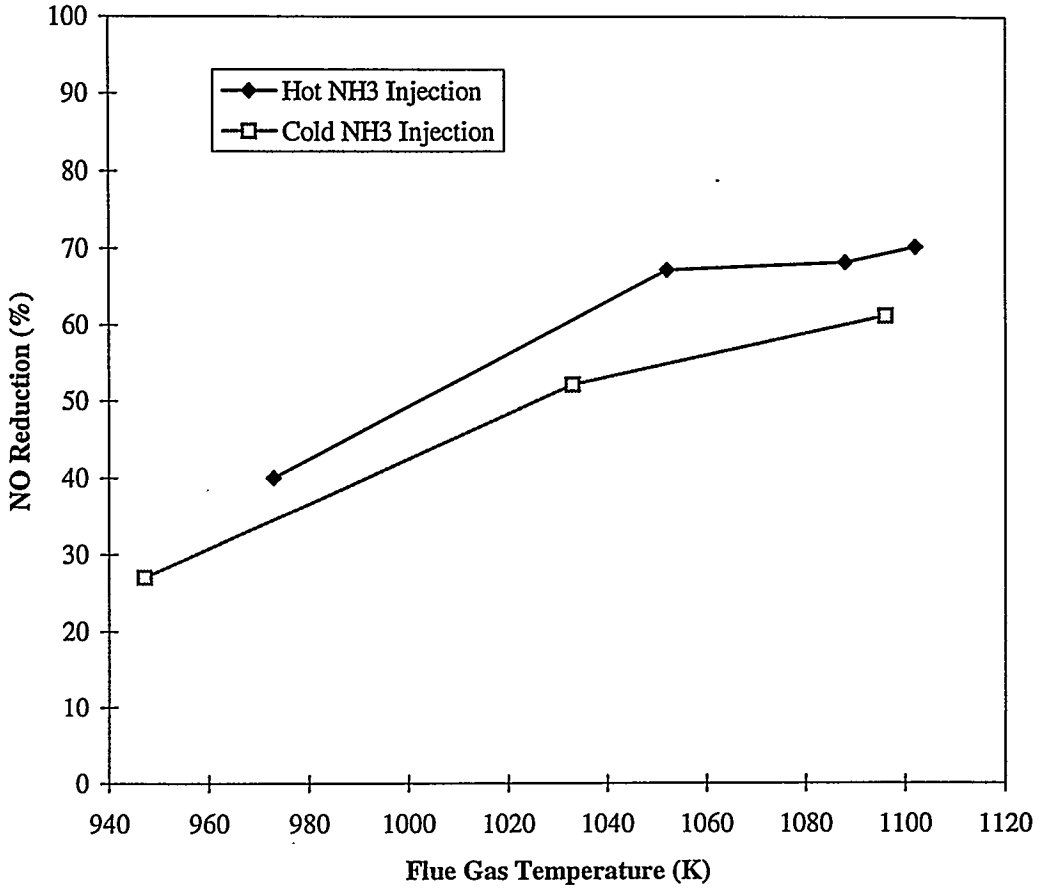

Figure 2.4: Comparison of cold and hot injection NO reduction at 25% excess air conditions.

cold injection at all flue gas temperatures investigated, and NO reduction increased with combustion temperature. Of note, the NH_3/NO_x ratio for this data varies between 5 and 7 over the range tested because the flue gas temperature was changed by altering the fuel and air flow rates without affecting the excess air. The difference between the two curves in Figure 2.4 is an indication of the thermal benefit of heating the ammonia before injection at these conditions.

To capture the actual benefit of generating ammonia radicals for injection using plasma technology, data from the previous plasma experiments were compared to hot injection data obtained under similar combustion and ammonia flow conditions. The plasma experiments by Zhou et al. were not used to explore the effect of flue gas temperature on NO_x reduction, so the data relevant to such a comparison with hot ammonia injection are sparse. Multiple data points for NO_x reduction at the same excess air condition but different combustion temperatures were found for 0% excess air only. Figure 2.5 shows results for NO reduction at 0% excess air plotted

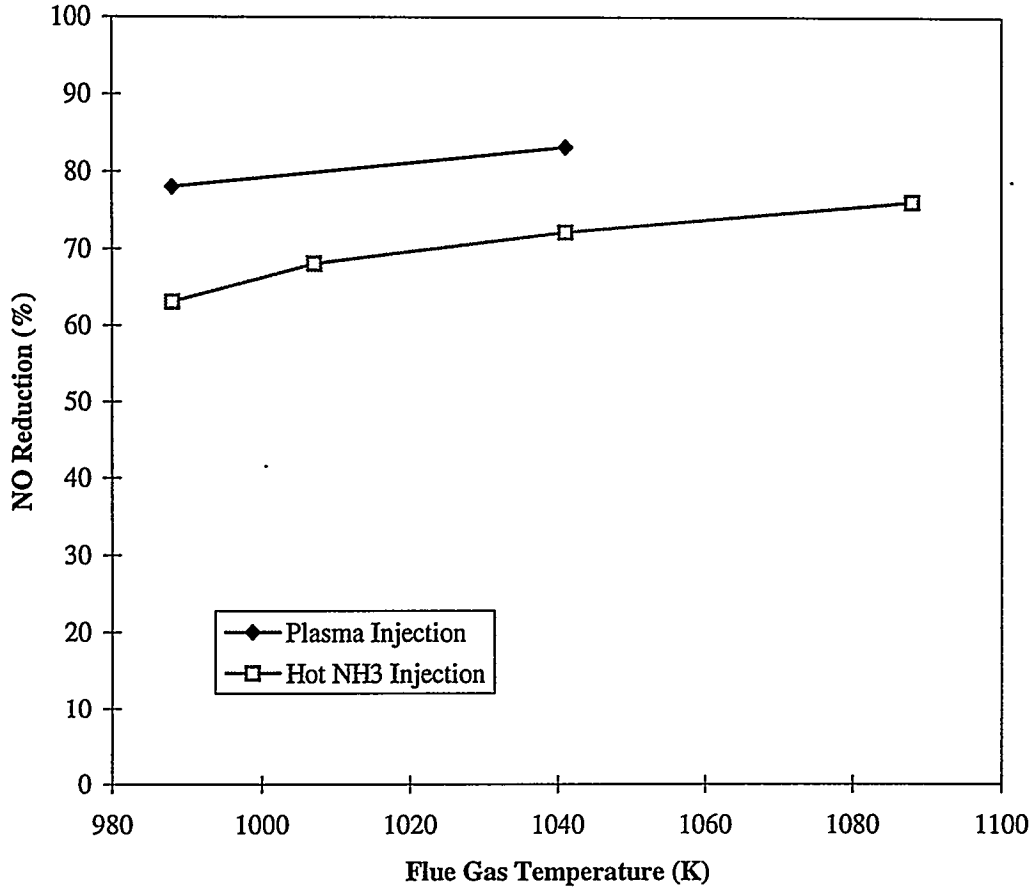

Figure 2.5: Comparison of hot and plasma-assisted injection NO reduction at 0% excess air conditions.

against combustion flue gas temperature. The combustion temperature was not reported in the plasma experiments, and so it is assumed that the temperatures found in the hot injection experiments at the same fuel and air conditions apply. This is consistent with reports by Zhou et al. that the plasma injection process did not affect the temperature below the injection point. The difference between the two curves in Figure 2.5 indicates that there is a benefit to externally generating ammonia radicals that is due to the interaction with the plasma and is beyond the bulk thermal benefit of hot injection.

While the lack of plasma experiment data precluded making further comparisons between plasma and hot ammonia injection over a range of flue gas temperatures holding other conditions constant, direct point comparisons between the two sets of data give insight into the NO_x reduction effectiveness of each under identical conditions. In this way, the relative contributions of thermal and plasma effects can be clearly seen in Figure 2.6. The plasma experiment data

provided four points in which all conditions were held constant except for the air flow rate. These conditions were duplicated using both hot and cold injection, leading to direct point comparisons among hot NH_3, cold NH_3, and radical injection at four excess air conditions. Since the combustion temperature increased with decreasing excess air (the same amount of fuel was used in all four cases), the difference between the NO reduction values in the columns in Figure 2.6 include two separate effects. However, between the 0% and 25% excess air conditions, which is a typical range for commercial boilers, the flue gas temperature increase was no more than 16 K, indicating that the excess air condition itself was the dominant variable. The average combustion temperatures at 75%, 50%, 25%, and 0% excess air were 922 K, 938 K, 960 K, and 976 K, respectively. The data for hot, cold, and radical injection in each column were obtained for identical gas flow conditions. For each condition, the fraction of the total NO reduction attributable to each effect is indicated by the relative sizes of the shaded sub-regions compared to the overall column height. As shown, NH_3 injection was more effective at lower levels of excess air. The effect of heating the NH_3 before injection was negligible at 50% and 75% excess air, but became significant at 25% excess air and more so at 0%. In contrast, the contribution of the use of the plasma generator to NO reduction was largest at the higher levels of excess air. This plasma effect contribution was offset by the thermal effect at lower amounts of excess air, but was still significant in all cases.

Discussion

At excess air conditions typical of utility and industrial boilers, the extra NO_x control achieved by heating the NH_3 before injection ranged from 2-15%, depending on the ammonia flow rate. At NH_3/NO_x ratios typical of SNCR applications, the extra NO_x control achieved by heating the NH_3 before injection appears to be modest. However, the cost of such a modification may also be modest, depending on how the ammonia or other agent is delivered to the flue gas. Some SNCR processes inject ammonia or urea as a liquid spray[11] into the flue gas stream. For safety reasons, heating of this spray would have to occur just before injection. For example, a small amount of flue gas or steam could be diverted into the stream near the injection point, or the injector could be heated in some manner, although this may require modifications to handle the phase change of the ammonia spray. A further investigation into the cost of such

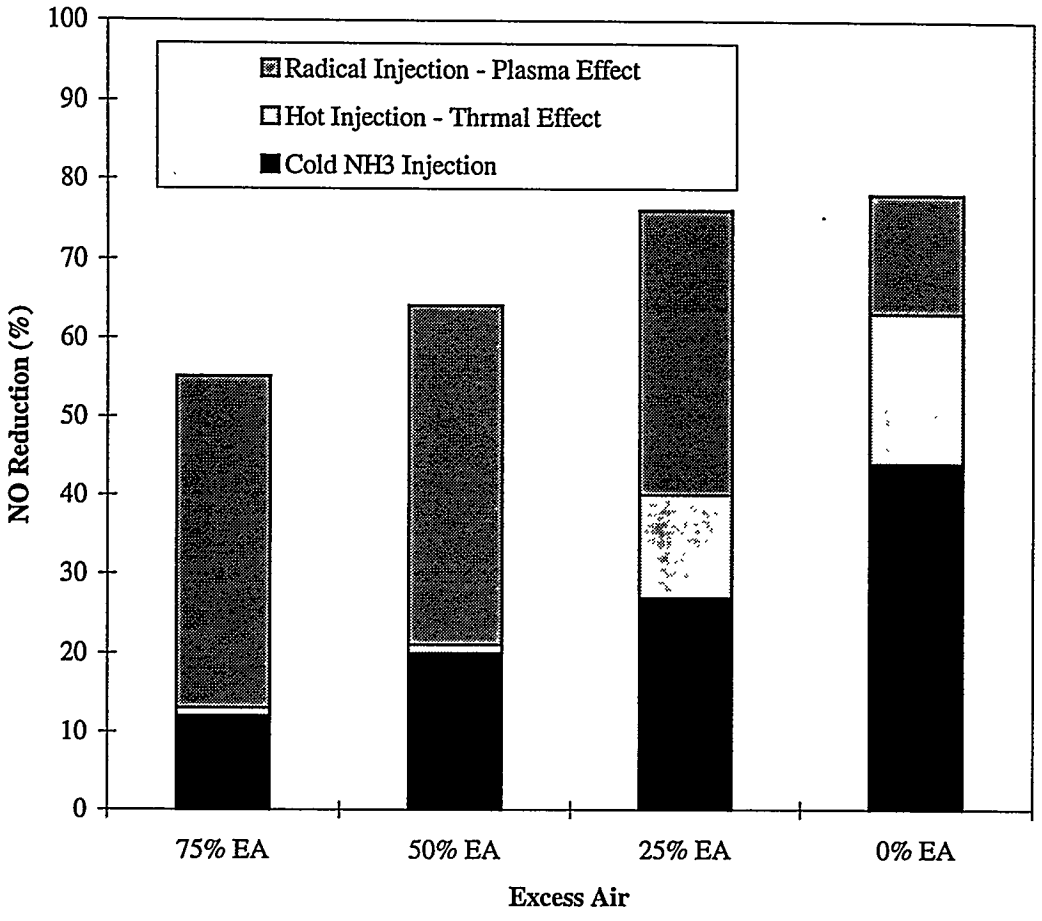

Figure 2.6: Point comparisons for cold, hot, and plasma injection under identical gas flow conditions.

modifications is worthwhile, particularly in applications where only a minor improvement in emission control is required.

Hot SNCR processes do not appear to have the potential to achieve NO_x control comparable to that seen in SCR applications or the plasma injection experiments. The lab-scale plasma experiments resulting in SCR-typical NO_x reduction were conducted at NH_3/NO_x ratios not seen in applications of other post-combustion NO_x control techniques. However, at these conditions, it has been shown that the advantage of externally generating the ammonia radicals is significant. At excess air conditions between 0-25%, the plasma effect accounted for 15-35% additional NO_x reduction beyond any thermal benefit. Of note, while the plasma experiments generally used higher NH_3/NO_x ratios than those used in SCR or SNCR, the plasma studies found little or no excess ammonia discharge from their combustors[7,8] due to the destruction of

the ammonia in the radical generation process. Thus, ammonia slip may not be a concern, although high ammonia use would be expensive.

If a source requires 80-90% NO_x reduction, the choice between SCR and the plasma-assisted ammonia injection process may ultimately be a matter of cost. A preliminary study of the cost of the plasma process in a 200 MW utility boiler model application indicated that the annual costs of the plasma and SCR processes would be similar.[12] However, the study employed assumptions that would favor the plasma technology approach, particularly in using a high capital recovery factor and assuming an NH_3/NO_x ratio of 1.5. On the other hand, it based its cost estimates on year-round operation. One major difference between the two processes is that the capital costs for SCR are higher than its operating costs, while for the plasma system the opposite would be true. In areas like the northeastern United States where the ozone season is substantially shorter than the year, the plasma system could be operated part-time at substantial cost savings. The cost savings associated with part-time SCR control would be considerably less since the (dominant) capital costs are not avoidable. Thus, particularly under seasonal ozone control strategies, the plasma injection process for NO_x control may be cost-effective.

Conclusions

This chapter has focused on what contributions are made by thermal and plasma effects in the plasma-assisted ammonia injection process for NO_x control from combustion flue gases. To isolate the benefit due solely to the bulking heating of the ammonia, experiments were performed to determine the advantage of hot NH_3 injection over typical SNCR cold injection processes. It was found that heating the injection gases may provide a minor improvement in NO_x reduction at NH_3/NO_x ratios and temperatures typical of commercial SNCR applications. While the potential benefit may be small, it was suggested that the cost of making this modification to the existing technology may also be small. The benefit of hot injection increased as the NH_3/NO_x ratio was raised, but it is unlikely that the expense of additional ammonia use and the potential for ammonia discharge would be warranted to realize that benefit.

At NH_3/NO_x ratios used in the previous plasma experiments, there was a significant thermal effect associated with the high NO_x reduction reported by Zhou et al. at excess air conditions typical of commercial combustors. That is, a part of the NO_x reduction would have been achieved by higher temperature injection that did not use a plasma device to produce

ammonia radicals. However, the plasma effect was also significant, accounting for an additional 15% to 35% absolute NO_x reduction beyond any thermal benefit at typical excess air conditions. The advantage of external radical generation to achieve high NO_x reduction was more pronounced at higher excess air and lower temperature conditions.

It should be noted that no attempt has been made yet to optimize the plasma injection process for NO_x control. Given that the hot injection experiments indicated that the use of the plasma system is a real benefit beyond hot ammonia injection, optimization of the process should either increase this benefit or decrease the cost of achieving the same NO_x reduction. The remaining chapters focus on developing a better understanding of the parameters that affect plasma deNO_x performance.

Chapter 3: Opposed Flow Experiment

Introduction

The plasma-assisted ammonia injection process is diffusional in nature, involving the mixing of the radical gas stream with the combustion flue gas. At the interface of these two streams, the NO_x reduction reactions occur. Because the interface is turbulent and the reactions are at non-equilibrium, the study of the fundamentals of the plasma deNO_x process is difficult. To study the fundamentals of plasma deNO_x at conditions relevant to the turbulent mixing process, an experiment using opposing laminar jets of plasma-treated gas and a NO_x-laden stream was designed and implemented. Laminar opposed flow reaction systems have been used in the past to investigate fundamental processes in turbulent diffusion flames,[13,14,15] because the system serves as a model for the eddy reactions in turbulent mixing layers. In addition, the use of an opposed flow system to investigate the plasma deNO_x process was designed to allow the investigation of the effects of different process parameters on NO_x reduction and the observation of plasma behavior.

Experiment Design

The main apparatus of the opposed flow experiment used to investigate the plasma deNO_x process is shown in cross-section in Figure 3.1 along with typical experiment parameters. The inductively coupled plasma torch used by Zhou provided the lower jet of ammonia radicals and argon carrier gas, while a hot tube arrangement identical to that described in Chapter 2 provided for the temperature control of the NO and N_2 gases comprising the upper jet. Each jet was emitted through a ceramic flow straightener measuring 6.3 cm in diameter, and the two jets were separated by approximately 2.5 cm. Temperature and NO_x concentration data were taken in the vicinity of the stagnation plane formed at the interface of the two jets, as well as throughout the mixing zone, using Chromel-Alumel (Type K) thermocouples and the Thermo-Electron Model 10AR NO/NO_x analyzer, respectively. The thermocouple probe measured 0.02 inches in diameter, and was cantilevered out of a ceramic holder for stability. The NO_x analyzer sample probe was constructed of 0.125 inch OD stainless steel tubing, which was flattened into an oval shape at the sampling end to allow for more accurate concentration readings vertically. Accurate

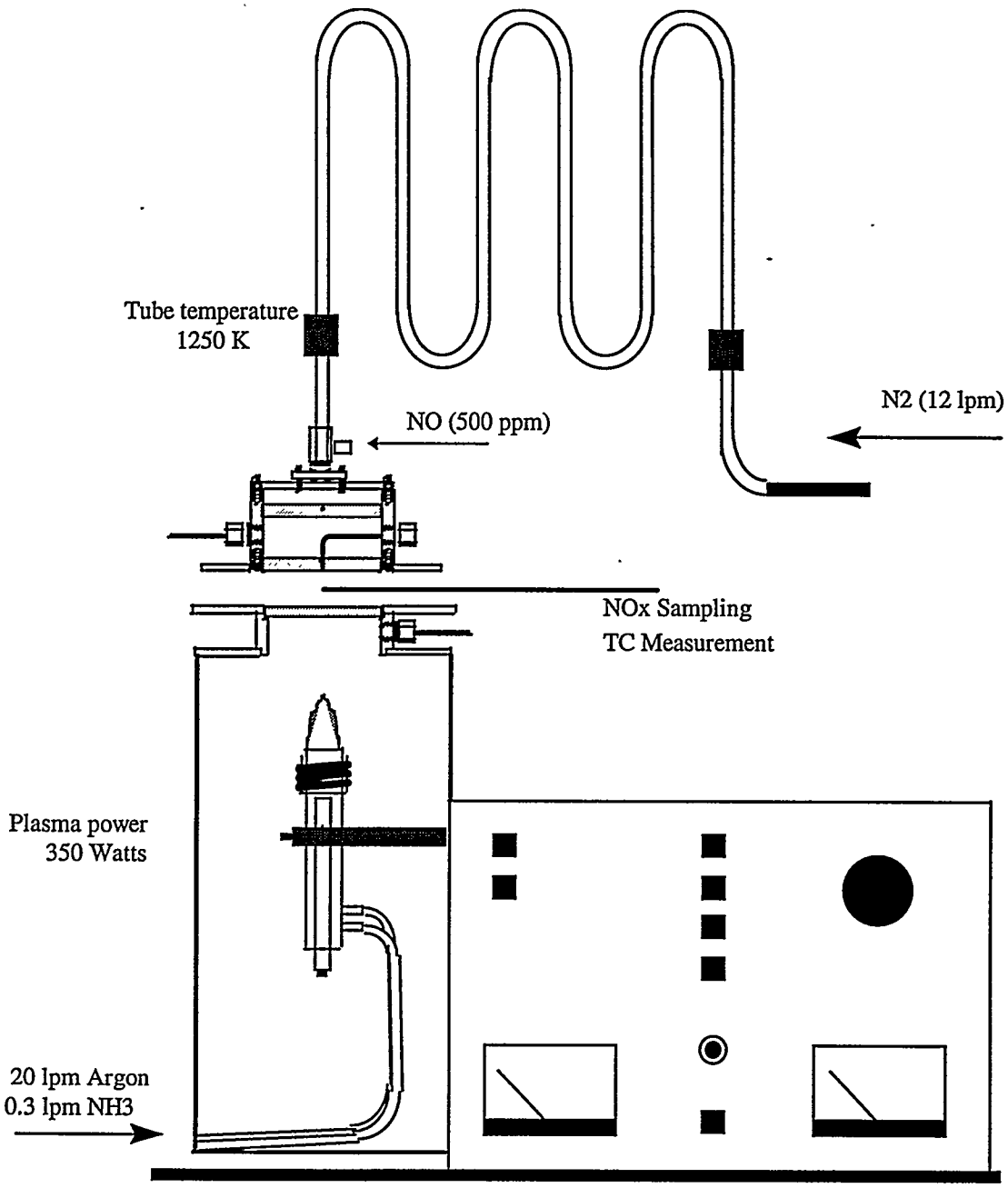

Figure 3.1: Opposed flow experimental apparatus.

positioning of the probes was accomplished with Velmex precision slide assemblies allowing for both vertical and 1-D horizontal translation.

Diagnostic testing of the opposed jets system included cold flow velocity measurements using hot film anemometry and hot flow temperature measurements to ensure the jets were laminar and properly aligned With the inclusion of the flow straightening ceramics, temperature readings fluctuated by only a few Kelvin and approximate Reynolds numbers based on the jet

diameters were less than 1000. Conditions chosen for testing the plasma deNO$_x$ process in the opposed flow experiment were based on the results of Zhou's work. The power supplied to the plasma ranged from 250 to 450 Watts, and the NH$_3$/NO$_x$ ratios (based on the approximate concentrations at the stagnation plane) were allowed to exceed typical SNCR ratios.

Results

During the diagnostic phase of the experiment, data indicated that the plasma can be a significant source of NO, particularly when operated in an air environment. Figure 3.2 shows the production of NO and total NO$_x$ (which includes NO) by the plasma as a function of plasma power when the device was operated in an air vs. an argon environment. The environment was controlled by bleeding 10 lpm of either gas into the plasma chamber. As shown, NO production increased with plasma power at a significant rate when operating in an air environment. This may be attributed to the dissociation of molecular oxygen and nitrogen and the subsequent formation of NO. Since the difference between the NO and NO$_x$ curves in Figure 3.2 is minor,

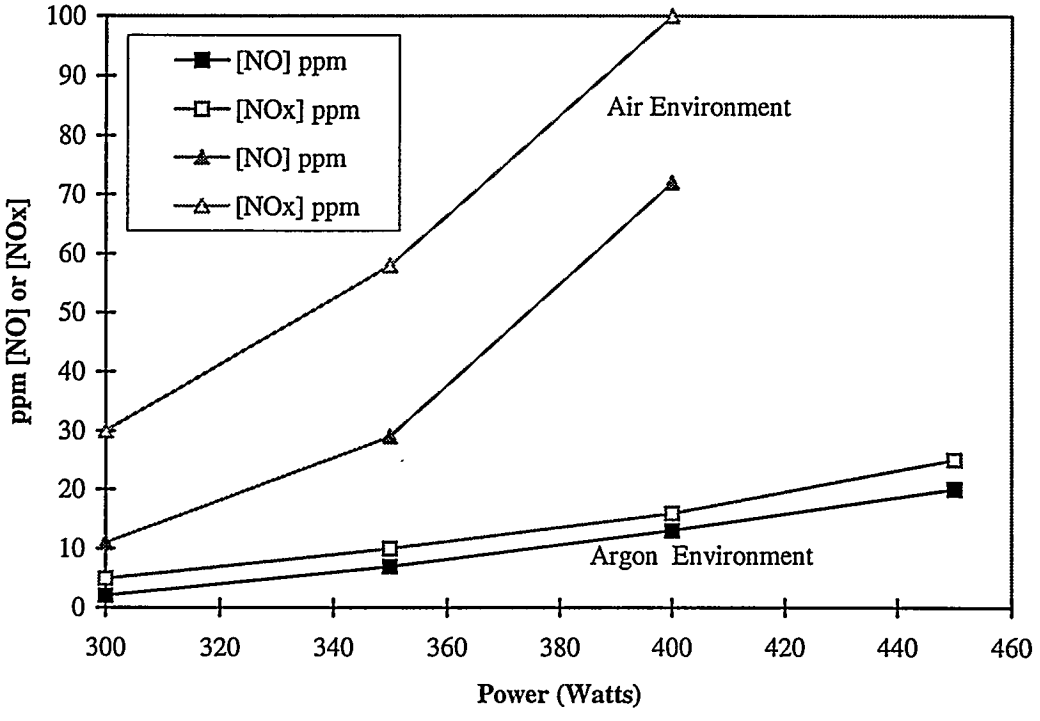

Figure 3.2: Pure argon IC plasma generation of NO and NO$_x$ in an argon vs. air environment.

the NO_x production shown was almost entirely nitric oxide.

Further, as shown in Figure 3.3, the NO production problem was exacerbated by initial addition of ammonia to the plasma. It is unknown what the exact mechanism for this production is, but the addition of NH_3 through the plasma represents an additional source of nitrogen atoms for NO production. However, with an increased addition of NH_3, the plasma seemed to be self-cleaning, reducing the NO back to near background levels. As a result of these diagnostic tests, all subsequent opposed flow experiments were run with 10 lpm argon gas being fed continuously into the plasma chamber.

A second characteristic of the inductively coupled plasma device was documented during the diagnostic phase, and this was a significant drop in temperature with NH_3 addition. Figure 3.4 shows the temperature at radial center in the opposed flow system at three vertical locations, near the top NO/N_2 jet (z = +1cm), at vertical center (z = 0cm), and near the bottom plasma-side jet (z = -1cm). The plasma was operating at 350 Watts during this experiment. As shown, the

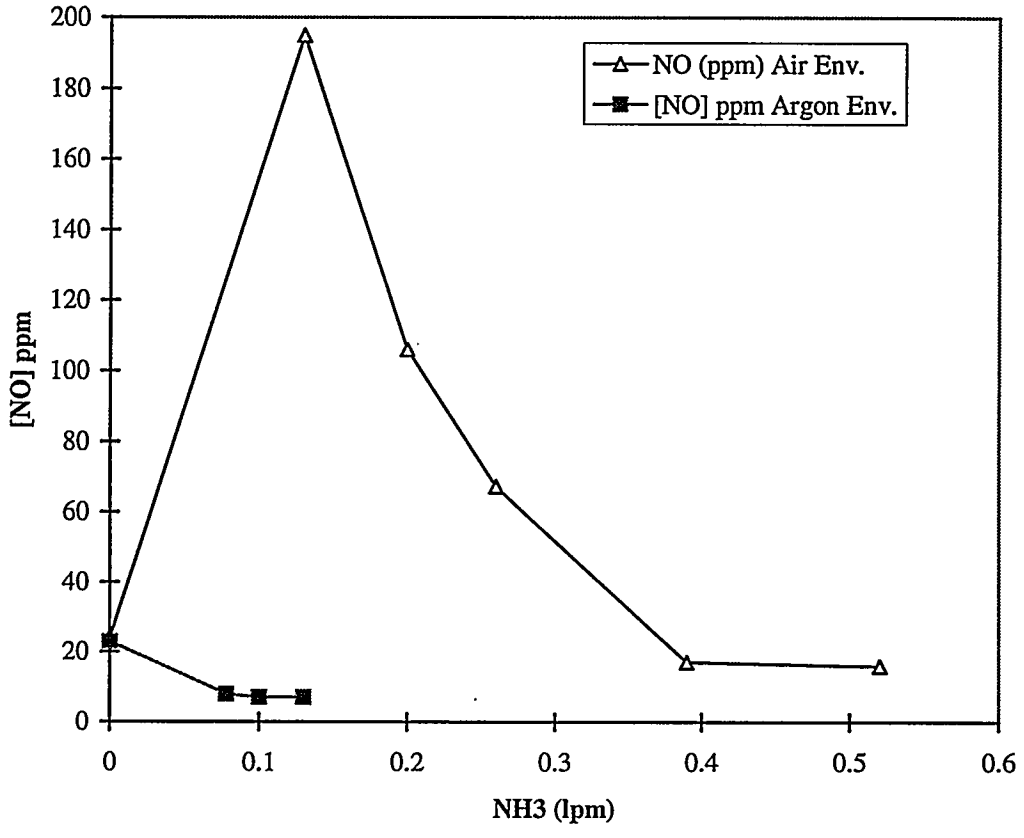

Figure 3.3: Effect of NH_3 addition on NO generation in IC plasma at 350 Watts.

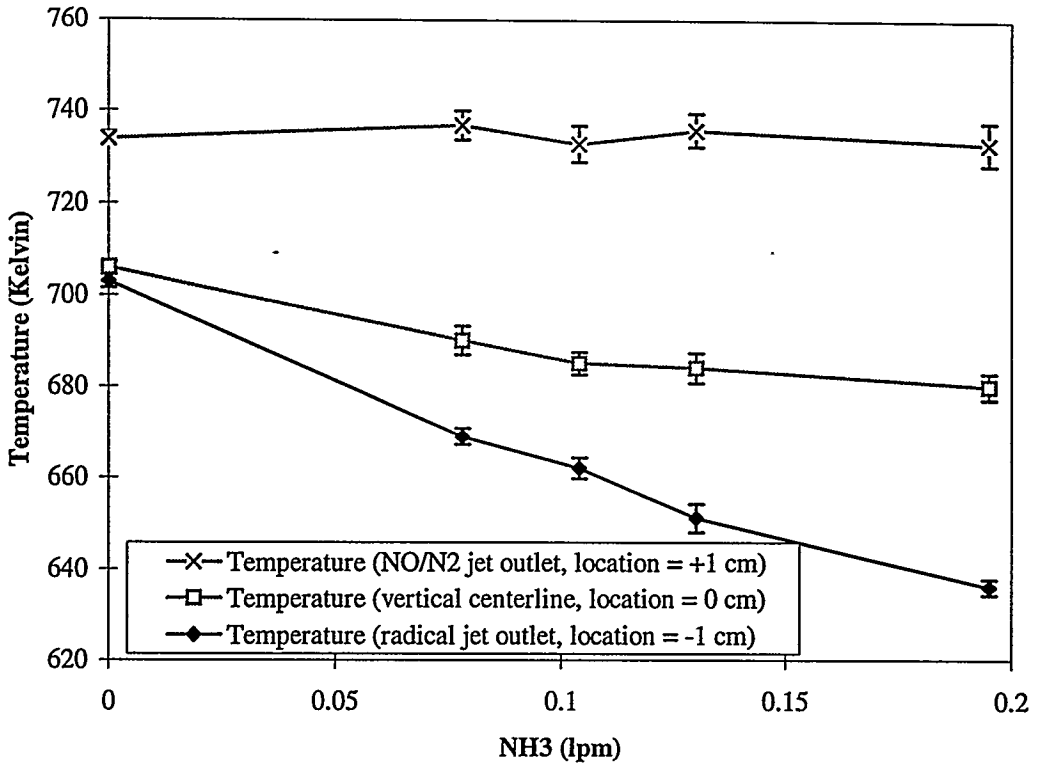

Figure 3.4: Temperature at three vertical locations in opposed flow system as a function of NH_3 flow rate, with IC plasma at 350 Watts.

top jet profile remains flat with NH_3 addition, but the increase in ammonia led to a decrease in temperature on the plasma side. This temperature change precluded the comparison of NO concentration levels at the same power with and without NH_3 addition because the vertical location of the stagnation plane would be shifted. In such a comparison, it would be unclear whether changes in the NO_x readings were a result of actual NO_x reduction or the shift in the opposed flow interface.

To counter this problem, an indicator for NO_x reduction was devised, as shown in Equation 3.1. The indicator uses the temperature measurements taken during the experiment as a surrogate for the degree of diffusion of one jet into the other. Since the NO_x reduction reaction does not produce heat, T^* is not affected by chemical reactions occurring in the system. (Note that the formula for T^* reverts to the form of the formula for NO^* if the gases from the top and bottom jets have the same C_p.) By comparing the NO concentration at a certain vertical location to the concentration that would be expected by diffusion alone, the value computed in Equation 3.1 "indicates" the degree of NO_x reduction at that location. A value of 1 would mean that no

NO_x reduction occurred, while a value of zero indicates complete NO_x reduction. The scale is linear between these two values.

$$NO^* = \frac{NO - NO_{bottom}}{NO_{top} - NO_{bottom}} + 1$$

$$T^* = \frac{C_{p,bottom}\left(T - T_{bottom}\right)}{C_{p,bottom}\left(T - T_{bottom}\right) + C_{p,top}\left(T - T_{top}\right)} + 1 \qquad \textbf{Equation 3.1}$$

$$\text{Indicator} = \frac{NO^*}{T^*}$$

Data taken during the opposed flow experiment at 350 Watts was reduced using Equation 3.1, and the results are shown in Figure 3.5. If significant NO reduction had occurred, the values

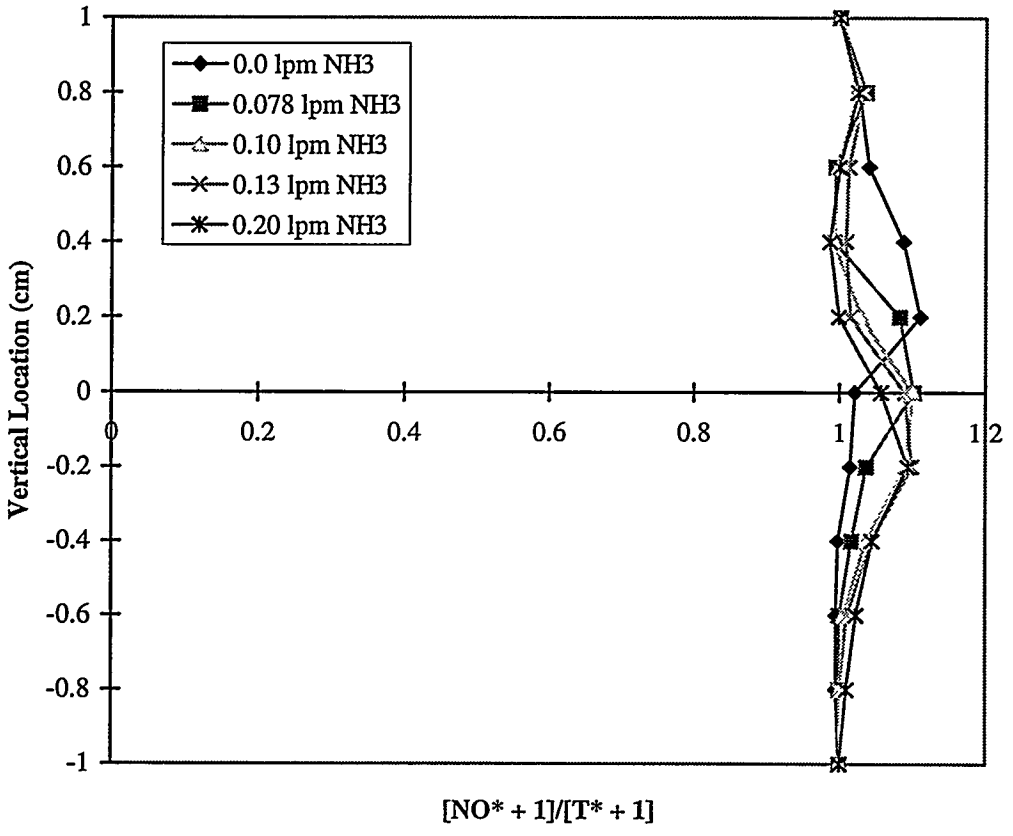

Figure 3.5: Typical opposed flow experiment results. NO*/T*, an indication of NO_x reduction if less than 1, is shown as a function of vertical position for various NH_3 amounts at 350 Watts.

of the indicator would have fallen significantly below 1. As shown, no significant NO_x reduction was recorded.

Discussion

The data in Figure 3.5 were recorded at 350 Watts, below the power used by Zhou for her best demonstration experiments, and it was shown in Chapter 1 that lower power led to better NO_x reduction. It is therefore believed that the plasma power used in the opposed flow experiment was appropriate. In comparing the ammonia used in the two experiments, the highest NH_3 addition in Figure 3.5 represents an NH_3/NO_x ratio of approximately 13, roughly twice that necessary for successful results by Zhou. However, due to the smaller scale of the opposed flow experiment, the actual flow rate of NH_3 through the plasma in the opposed flow experiment was approximately four times less than used by Zhou in her best NO_x reduction conditions. At more comparable conditions, specifically 0% excess air and an NH_3 flow rate of 0.23 lpm, Zhou's data indicate that NO_x reduction would still be expected, but only 33% at 350 Watts. Thus, it is apparent that understanding the interaction of the plasma with the NH_3 as a function of NH_3 flow rate is important to understanding the success of the demonstration experiments.

A second significant difference between the opposed flow and demonstration experiments is the temperature at which the NO_x reduction reactions would be carried out. In Zhou's experiments, the temperature in the combustor at the plasma injection point was roughly 1000 Kelvin, depending on the excess air conditions. In contrast, due to several design constraints, the temperature in the opposed jet system did not exceed 800 Kelvin. Among the constraints limiting the opposed flow system were the need to operate the plasma at lower power (and therefore lower temperature), the limitations of the hot tube system, and – most importantly – the need to allow space for the use of flow straighteners to achieve smooth, laminar velocity profiles in the two jets. By allowing space for the straighteners, significant heat loss was incurred. In addition, it is possible that the straighteners could act as scavenging surfaces for the ammonia radicals.

Due to the limitations of the opposed flow experiment, a new experiment was designed specifically to allow the exploration of the temperature limit of the plasma deNO_x process, as well to verify the effects of plasma power and NH_3 flow rate on the process. This experiment is

described in Chapter 4. Briefly, the new experiment involves the injection of a NO/N_2 stream directly toward the plasma. In this experiment, the ability to simulate the turbulent eddies with the laminar opposed flow system is lost. However, the temperature limitation is significantly reduced by eliminating the flow straighteners and moving the NO/N_2 injection to within centimeters of the plasma torch (the torch itself is used as the heat source to set the injection temperature).

Conclusions

The opposed flow experiment failed to demonstrate the effectiveness of plasma $deNO_x$ injection at the conditions tested. Chapter 4 will describe the subsequent "reverse injection" experiment that achieved significant NO_x reduction, explored the temperature limit of the plasma $deNO_x$ process, and verified the effect of plasma power and NH_3 flow rate on process performance. Chapter 5 will then present the results of chemical kinetic modeling and a survey of current plasma modeling capabilities that are applicable to the plasma $deNO_x$ process.

The opposed flow experiment, however, did show several characteristics of the IC plasma system of practical importance if applied to the plasma $deNO_x$ process. It was shown that the plasma can be a significant source of NO if operated in ambient air. The initial addition of NH_3 passed through the plasma operating in an air environment led to an increase in NO concentrations, but subsequent NH_3 addition demonstrated that the plasma appears to be "self-cleaning." It was also shown that the temperature of the plasma decreases with NH_3 addition. This likely leads to a change in the radicals produced as more NH_3 is added. This effect is considered again in Chapter 5.

Chapter 4: Reverse Injection Experiment

Introduction

To counter the limitations of the opposed flow experiment, a new experiment was constructed and implemented. This experiment involved injecting the NO-laden stream toward the plasma, instead of injecting the plasma into the NO-laden gases, and so it will be referred to as the reverse injection experiment. The new set-up allowed for the exploration of the lower limit of the NO-stream temperature that still led to significant NO reduction with the plasma deNO$_x$ process. In addition, the effects of NH_3 amount and plasma power were investigated.

Experiment Design

Figure 4.1 shows the reverse injection experimental set-up. The plasma chamber from the opposed flow experiment was modified by replacing the flow straighteners required for the radical jet with a short (approximately 25 cm) stack. A 1/8" OD stainless steel tube for injecting an NO/N_2 gas stream was mounted vertically to a translating slide and aligned for movement down the center of the stack. During operation, the temperature of the NO/N_2 injection stream was controlled by moving the injector closer or farther from the plasma torch. This required moving the injector inside of only a 3 cm range during typical operation, with the lowest probe position perhaps 4 cm from the plasma tip. The temperature at the injection point was monitored with a Chromel-Alumel (Type K) thermocouple probe. At the top of the stack, a sampling probe leading to the Thermo-Electron Model 10AR NO/NO$_x$ analyzer was used for NO$_x$ concentration measurements. This probe was mounted to a slide for horizontal translation for taking radial NO$_x$ concentration profiles.

During the experiments, the plasma was operated between 250 and 400 Watts with 0 to 0.65 lpm NH_3 passing through it. Similar to Zhou's experience, the lower powered plasmas were restricted to lower ammonia flow rates to maintain plasma stability. A constant feed of 10 lpm argon gas was delivered into the plasma chamber to keep the plasma in an oxygen-free environment and avoid any NO production. The argon flow rate through the plasma was 20 lpm through the outer line (Q_3 in Figure 1.1) in most of the experiments (except where noted) and 1.5 lpm through the inner line (Q_2 in the same figure) at all times.

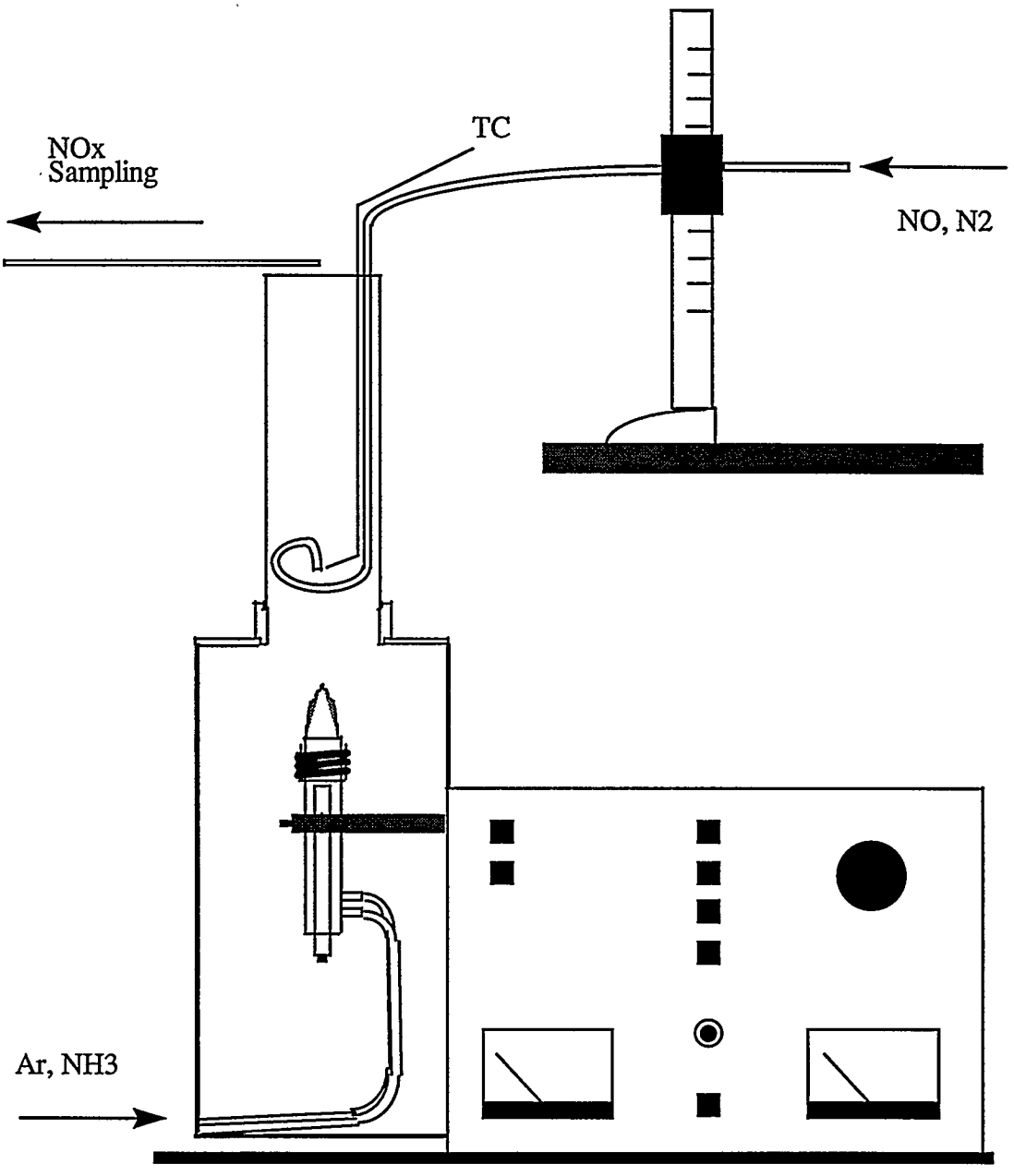

Figure 4.1: Reverse injection experimental set-up.

Results

Results for NO_x reduction in the reverse injection experiments are presented in decreasing order of plasma power, with comparisons between results at different powers given afterwards. At 400 Watts, the power at which almost all of Zhou's demonstrations were conducted, modest NO_x reduction was recorded at the highest NH_3 flow rate used (0.65 lpm). Figure 4.2 presents the results as the fraction of original NO (without NH_3 addition) remaining as a function of

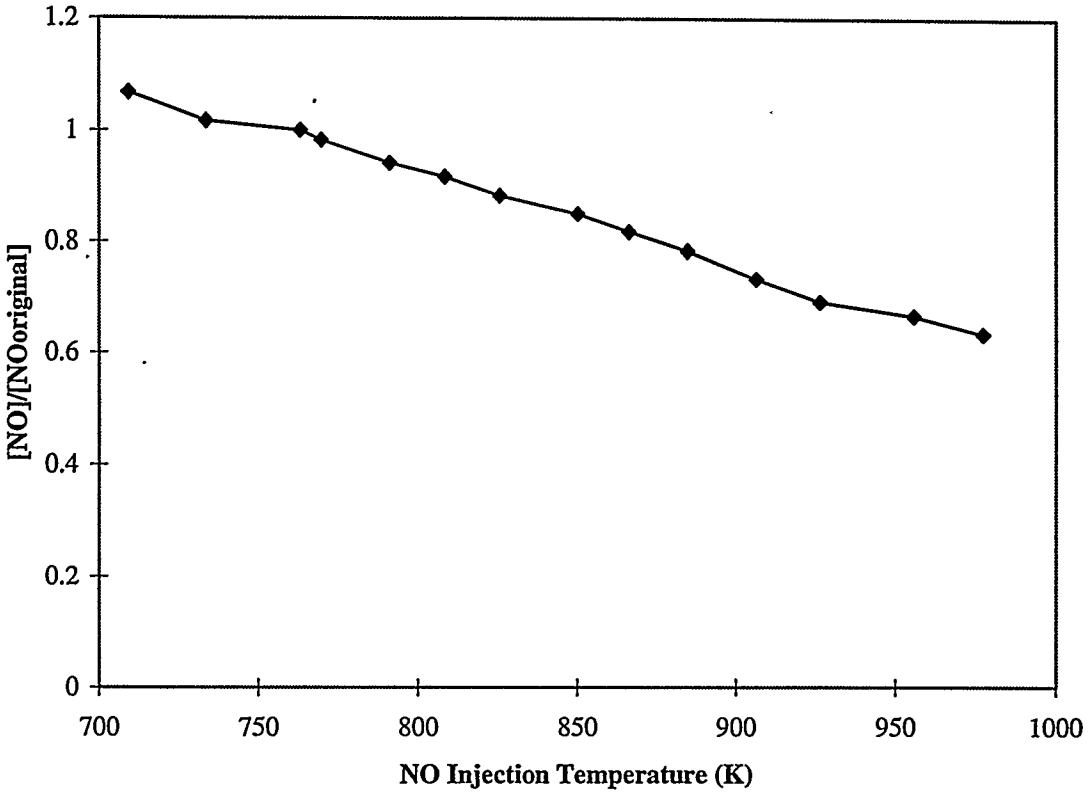

Figure 4.2: NO/NOinitial, with plasma at 400 Watts, 25 lpm main argon flow rate, and 0.65 lpm NH_3, vs. NO/N_2 injection temperature.

injection temperature. As shown, reduction was improved by increasing the injection temperature, although at the highest temperature tested only 37% NO reduction was recorded. Of note, the test temperature was increased by moving the injector closer to the plasma until the plasma was extinguished. It is believed that the loss of plasma stability was due to interference of the metal thermocouple probe and NO/N_2 line with the magnetic field produced by the inductance coil, although this is conjecture.

The results at 400 Watts were at an NH_3/NO_x ratio of 29, clearly indicating that the fate of the NH_3 as it is passed through the IC plasma at these conditions was not the efficient production of NO-reducing radicals. However, several differences between these results and Zhou's work done at the same plasma power should be highlighted. First, Zhou used even higher amounts of NH_3 through the plasma (up to 1 lpm), although due to the scale of her experiments the NH_3/NO_x ratio at these conditions was only about 9. As was shown in Figure 3.4 and will be highlighted again later, the NH_3 flow rate through the plasma had a significant effect on plasma temperature, which would in turn affect the radicals produced. A second difference between the

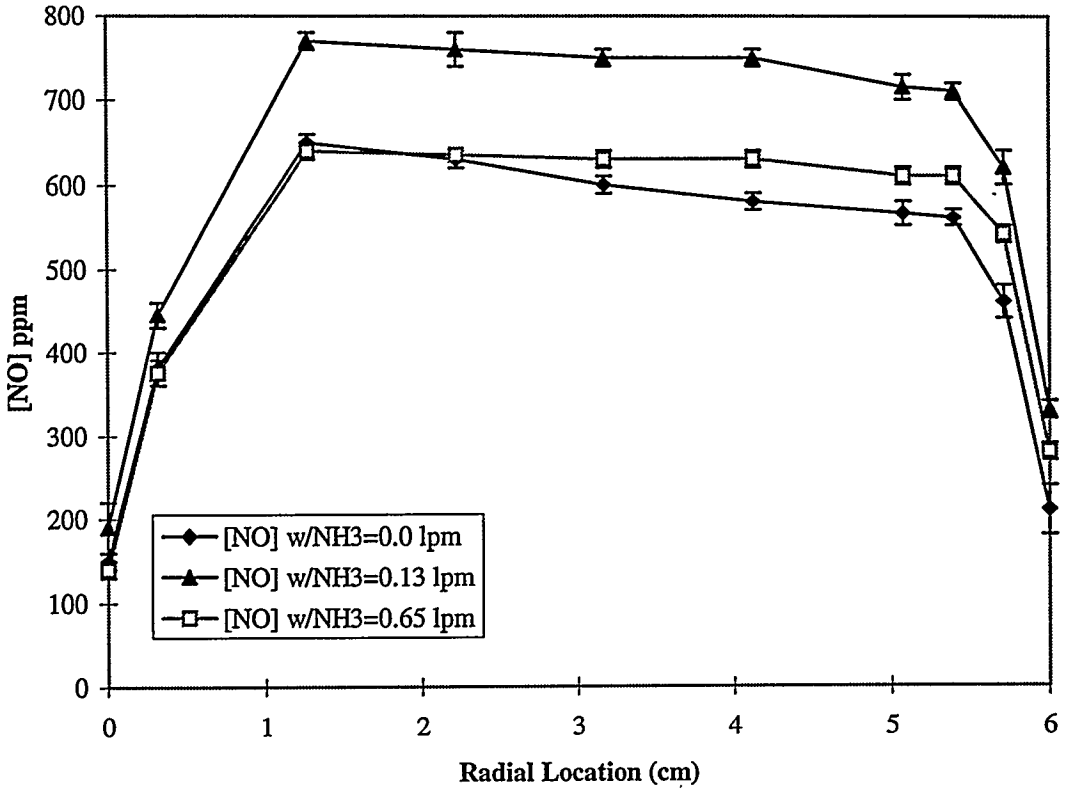

Figure 4.3: Radial NO concentration profiles taken across the reverse injection stack for a 400 Watt plasma.

demonstration work and the present experiment is the allowed reaction time. Given the dimensions and average flow rates within the demonstration experiments, a reaction time of several seconds is expected, while due to the smaller scale of the reverse injection experiment, a reaction time of less than one second is expected. While direct radical reactions would occur well within this timespan, the extra reaction time in Zhou's experiments would allow unspent ammonia or other NO_x reducing agents to break down and react before sampling occurred (much as it occurred in the hot NH_3 injection experiment described in Chapter 2). Since the reverse injection experiment was meant to explore the parameters affecting plasma deNO_x performance, and since duplicating Zhou's work was not a priority, no modifications (such as a significantly longer and unwieldy stack height) were made to the apparatus.

One other curious result was achieved at 400 Watts, and duplicated at lower plasma power, and this was the apparent production of NO in the system with the initial addition of NH_3. Figure 4.3 shows radial profiles of NO concentrations for three levels of ammonia flow rate

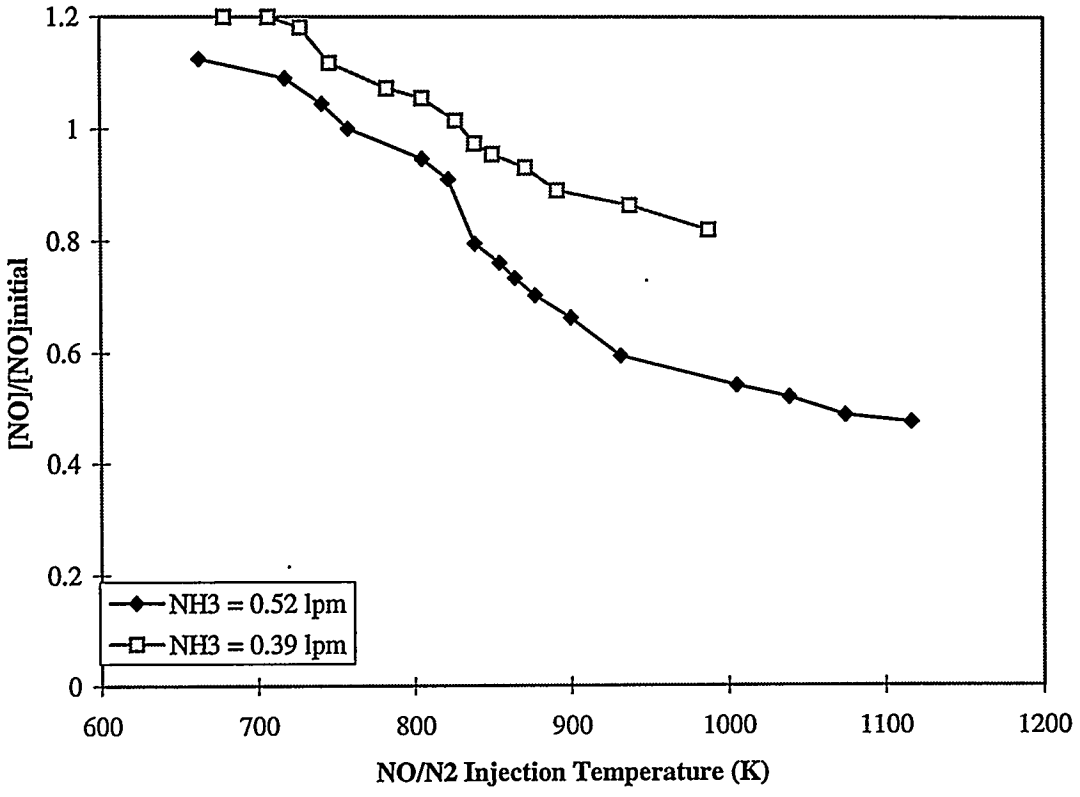

Figure 4.4: NO/NOinitial, with plasma at 350 Watts with 20 lpm main argon flow rate and two NH_3 flow rates, vs. NO/N_2 injection temperature.

through the plasma. These data were taken with the injection of NO/N_2 through the injector, with the purpose of examining the degree of mixing achieved at the stack exit. As shown, the NO concentration across the stack was uniform, but the value of the NO concentration increased with the addition of 0.13 lpm NH_3, and then recovered when the NH_3 value was increased to 0.65 lpm. Since the only oxygen in the system comes from the NO injection itself, it is suspected that the NO channel of the NO_x analyzer is reading some other species as NO. The precedence and mechanisms by which this could occur is presented in the Discussion section; however, it is noted here that this apparent interference would lead to conservative NO_x reduction results. All NO concentration results are presented as read from the NO_x analyzer, with no adjustments made for the apparent interference effect.

The exploration of lower plasma powers was a priority in the experiments, and Figure 4.4 shows results achieved at 350 Watts. As shown, NO reduction improved with injection temperature, as well as with the amount of NH_3 added through the plasma. Peak performance at 350 Watts was 53% NO reduction at the maximum achievable injection temperature of 1116

Kelvin, and with 0.52 lpm NH_3 flowing through the plasma. Higher ammonia flow rates proved to be unstable. Finally, at the lower ammonia flow rate, the interference effect was again observed.

The plasma power of 300 Watts was the lowest power that could be consistently sustained with ammonia passing through it, so considerable data were taken at this power. Figure 4.5 shows the injection temperature effect on NO reduction at three different ammonia flow rates. Similar to the results at the other powers, reduction improved with increasing injection temperature and ammonia flow rate. At this power, the amount of NH_3 needed to "erase" the interference effect was less than at higher powers. Peak performance at 300 Watts was 67% NO reduction at the maximum achievable injection temperature of 980 Kelvin, and with 0.39 lpm NH_3 flowing through the plasma. Additional NH_3 flow caused the plasma to extinguish.

Figure 4.6 shows the effect of argon flow rate through the plasma on NO reduction as a function of injection temperature. As shown, increasing the argon flow rate aided reduction,

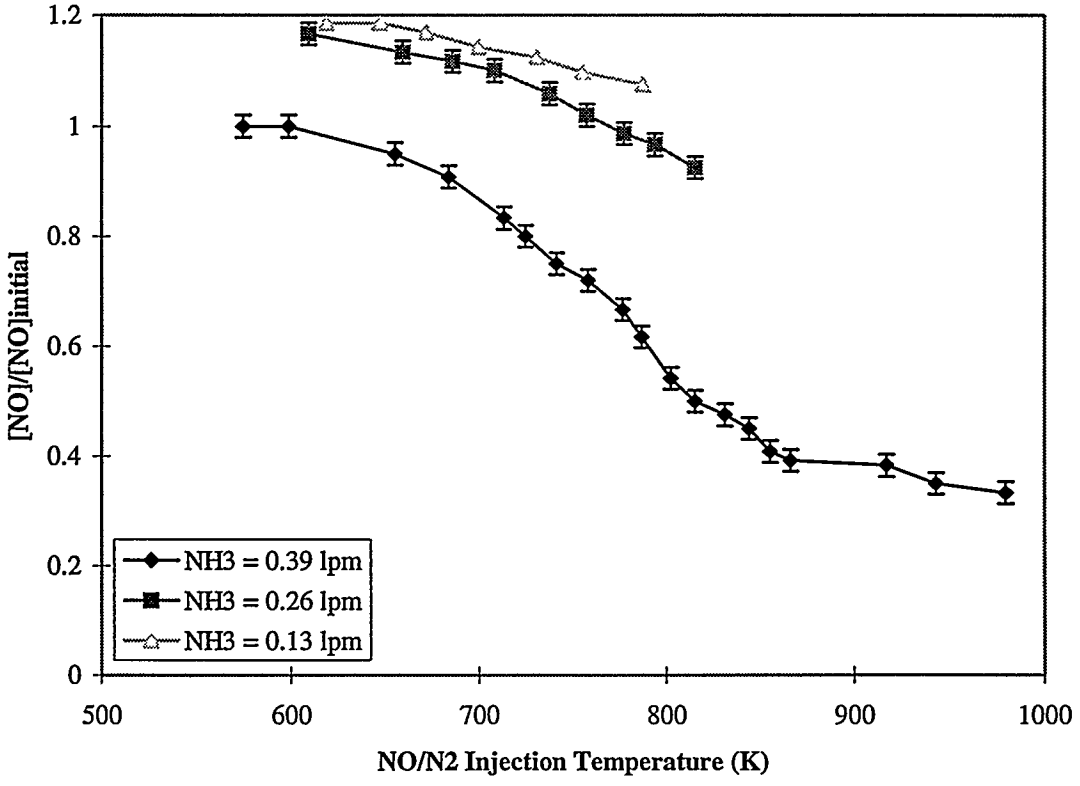

Figure 4.5: NO/NOinitial, with plasma at 300 Watts and 20 lpm main argon flow rate and three NH_3 flow rates, vs. NO/N_2 injection temperature.

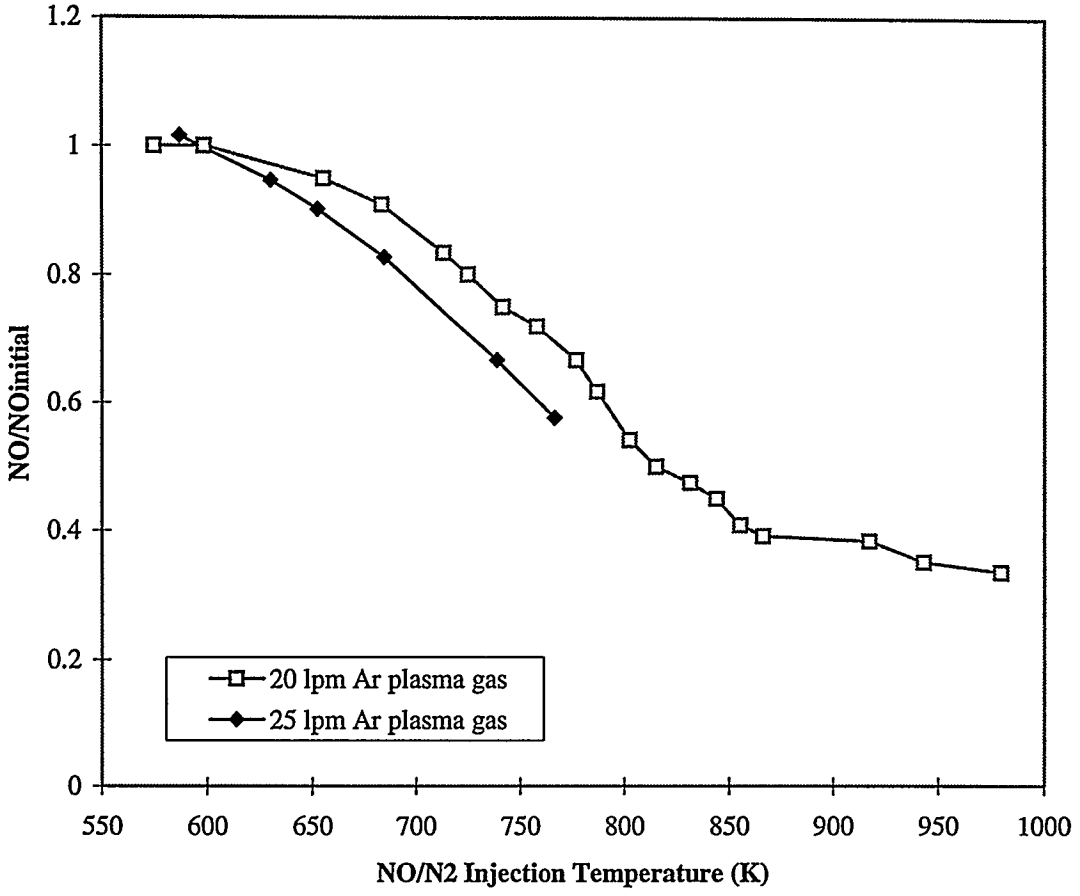

Figure 4.6: Effect of argon flow rate through plasma on NO reduction at 300 Watts as a function of injection temperature.

although increasing the flow rate also caused the plasma to blow out more readily. Figure 4.7 compares the NO reduction at similar injection temperatures as a function of NH_3 flow rate. The higher argon flow rate led to significantly better NO reduction at this relatively low injection temperature (~700 Kelvin).

At 250 Watts, the plasma was very difficult to sustain at even low ammonia flow rates; however, Figure 4.8 shows the effect of NO/N_2 injection temperature on NO reduction with 0.13 lpm NH_3 flowing through the plasma. At this low power and low ammonia flow rate, no apparent interference effect was recorded. Approximately 35% NO reduction was achieved at this power and flow condition at an injection temperature of 685 K.

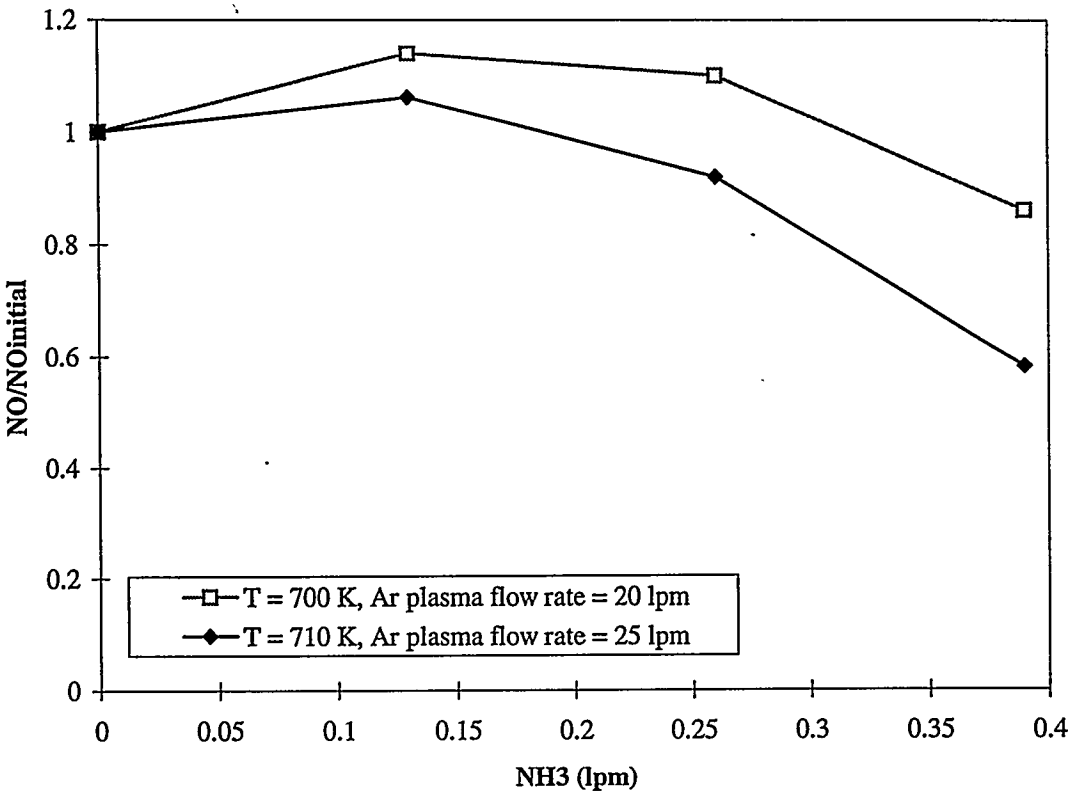

Figure 4.7: Effect of argon flow rate through plasma on NO reduction at 300 Watts and an injection temperature of approximately 700 K, as a function of NH_3 flow rate.

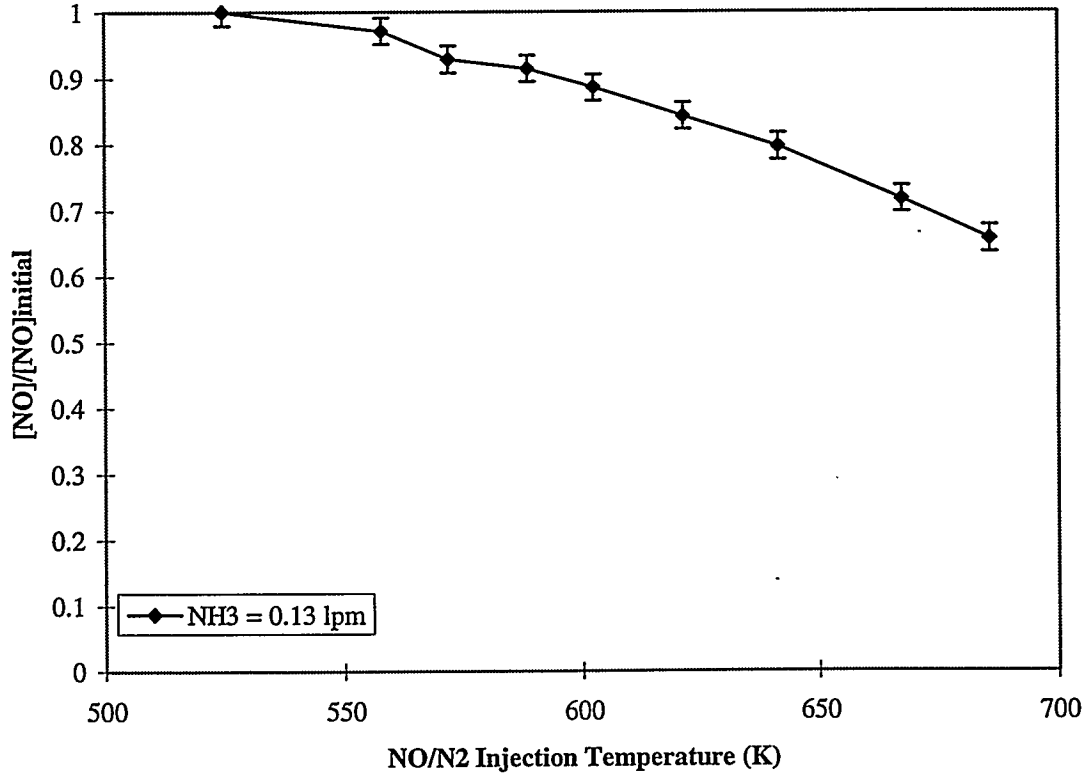

Figure 4.8: NO/NOinitial, with plasma at 250 Watts with 20 lpm main argon flow rate and 0.13 lpm NH_3 flow rate, vs. NO/N_2 injection temperature.

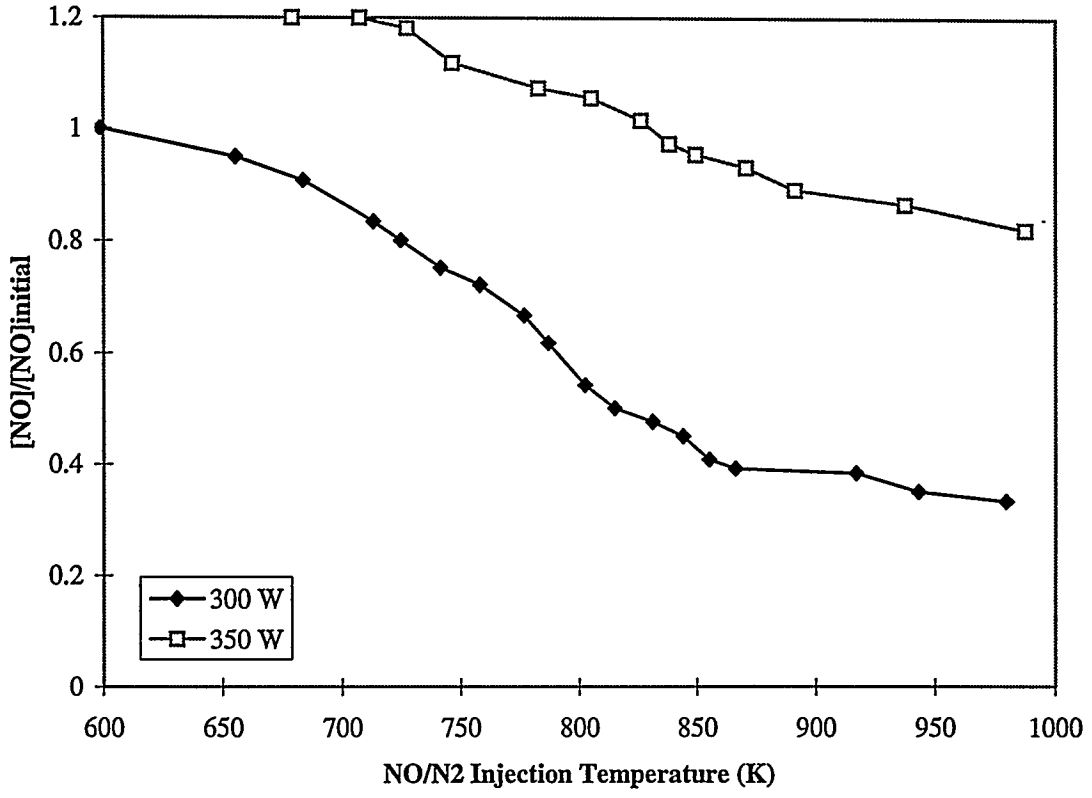

Figure 4.9: Comparison of plasma deNO$_x$ results under identical flow conditions with plasma power set to 300 vs. 350 Watts and an ammonia flow rate of 0.39 lpm.

Discussion

The results of the reverse injection experiment showed that the plasma deNO$_x$ process can be effective even when the temperature of the NO-laden stream is significantly below the necessary temperature window for SNCR. At both 300 and 350 Watts, most of the achievable NO reduction was completed at or below an injection temperature of 900 Kelvin. Particularly as shown in Figure 4.5 (at 300 Watts), increasing the temperature above 850 Kelvin led to only modest improvement, if any, in NO$_x$ reduction performance.

The plasma deNO$_x$ process also showed better NO$_x$ reduction at lower plasma power, when injection temperature and NH_3 flow rate were held constant. Figure 4.9 shows the comparison between performance at 300 and 350 Watts as a function of injection temperature with 0.39 lpm NH_3 flowing through the plasma. Figure 4.10 shows the same comparison between 250 and 300 Watts at the 0.13 lpm ammonia flow rate. In both figures, the lower power leads to better NO reduction for a given NO/N_2 injection temperature.

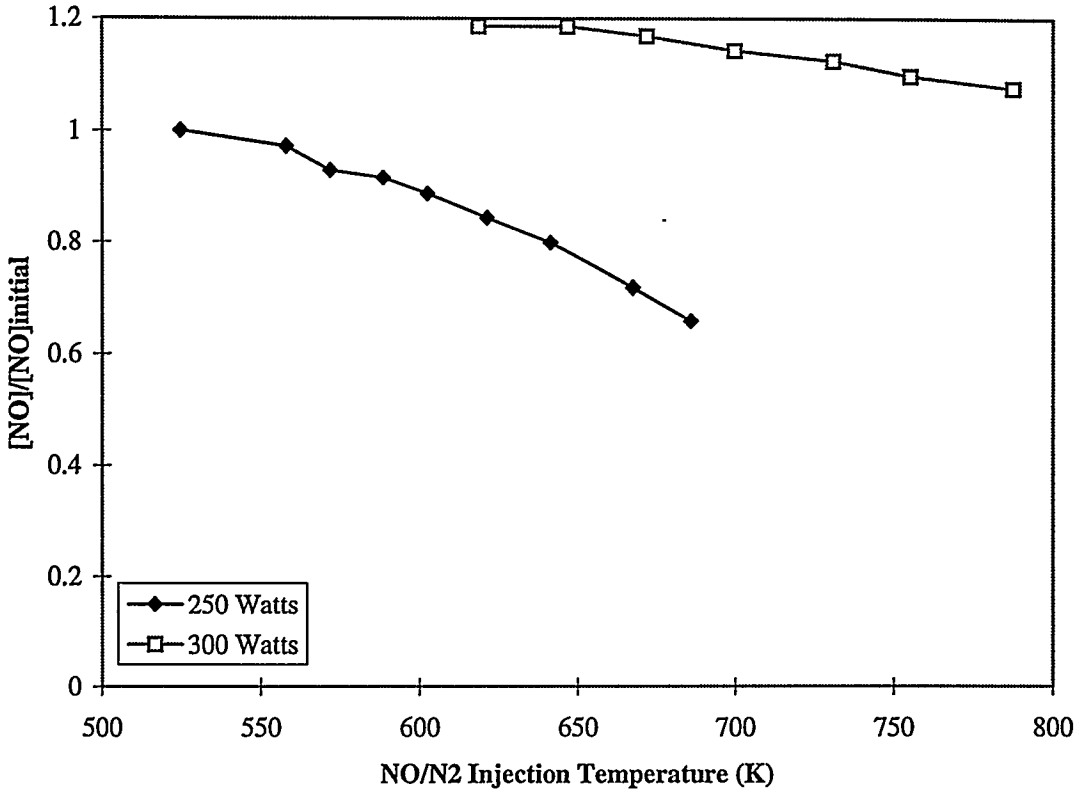

Figure 4.10: Comparison of plasma deNO$_x$ results under identical flow conditions with plasma power set to 250 vs. 300 Watts and an ammonia flow rate of 0.13 lpm.

Improvement in plasma deNO$_x$ performance also occurs with increased ammonia flow rate, although this is not surprising. Figure 4.11 shows the comparison of NO reduction at 300 and 400 Watts for an injection temperature of 710 Kelvin as a function of ammonia flow rate. As shown, the lower plasma power reduces more NO for a given ammonia flow rate, and more ammonia leads to better reduction. It is obvious that using more reagent should result in improved NO reduction. However, the mechanism for the improvement may also have to do with the drop in plasma temperature that results with increased ammonia flow. The amount of temperature drop is dependent on both the plasma power and ammonia flow rate, as shown in Figure 4.12. For 400 Watts, little drop in the plasma temperature is noted at the ammonia flow rates tested; however, the temperature of the 300 Watt plasma drops off sharply with ammonia flow rate. Of note, the 300 Watt plasma extinguished with any additional ammonia, but the 400 Watt plasma was still stable at the conditions tested.

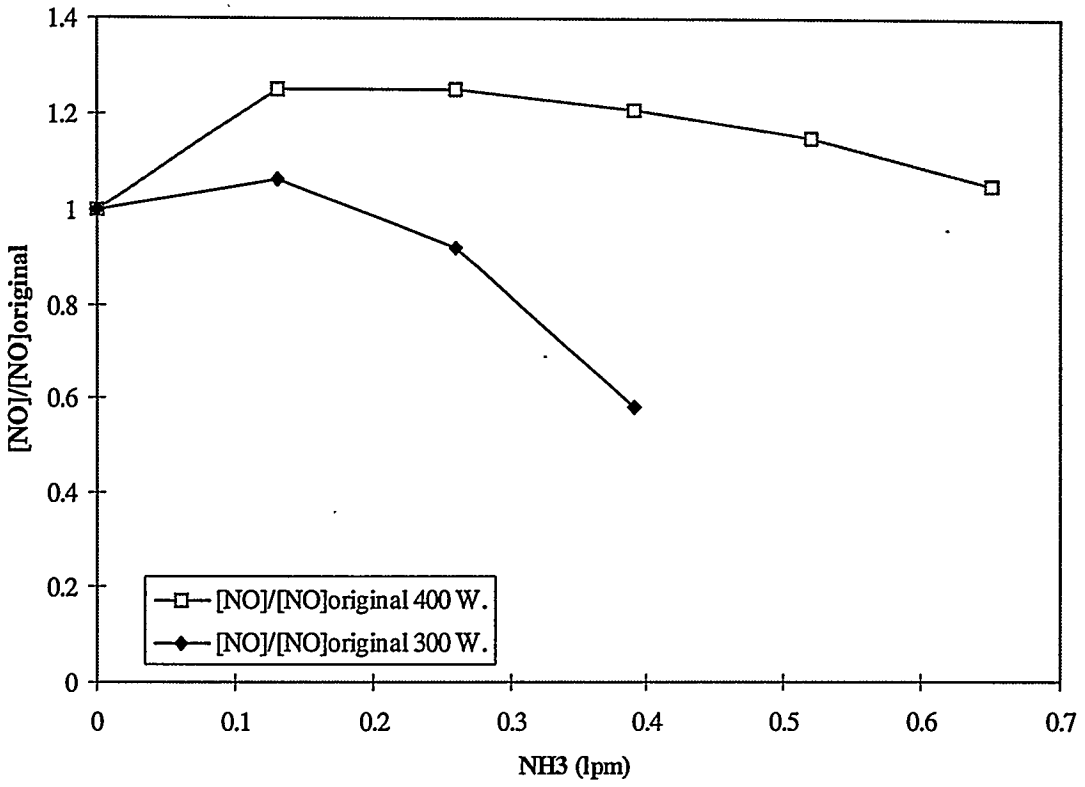

Figure 4.11: NO reduction at 300 and 400 Watts as a function of ammonia flow rate at a 710 K NO/N_2 injection temperature.

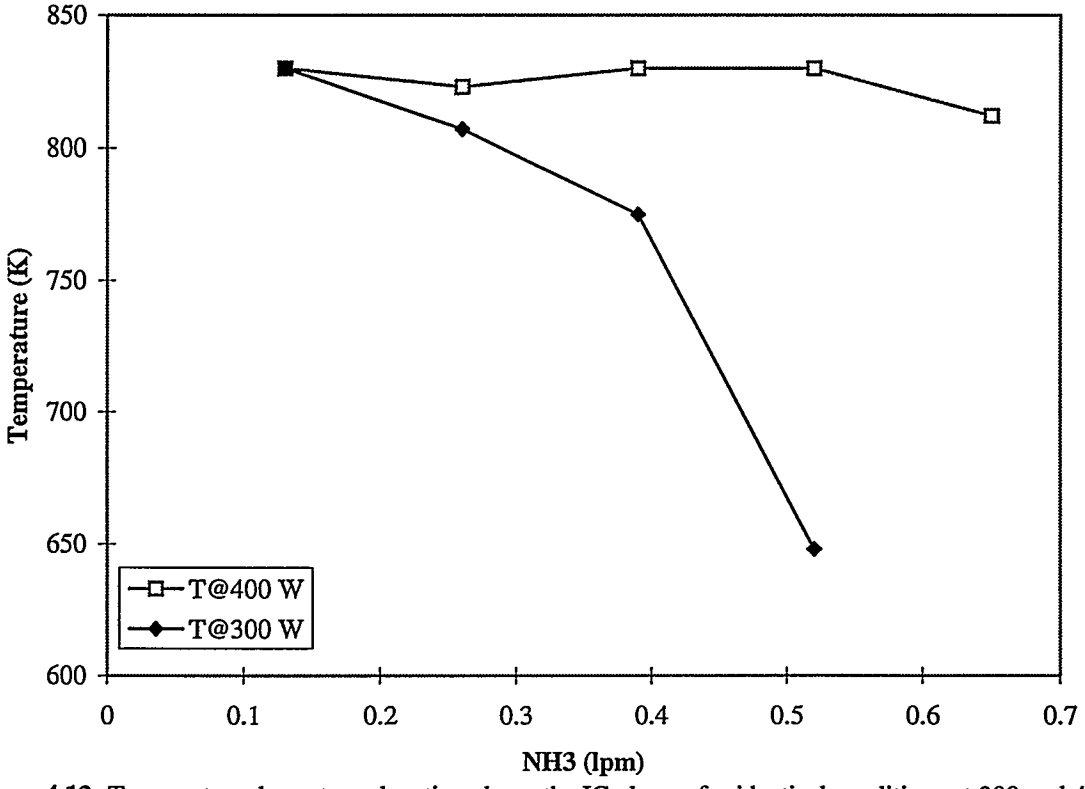

Figure 4.12: Temperature drop at one location above the IC plasma for identical conditions at 300 and 400 Watts.

The interference of other species produced by the ammonia-doped plasma on the NO readings taken during the experiments was particularly troublesome. Tests with the pure argon plasma failed to produce significant NO readings when the plasma was operated in an argon environment, which would indicate that little oxygen remained in the system under those conditions. With no additional oxygen source besides the injection of baseline NO, reading other species erroneously as NO is the most likely explanation for the apparent NO "production." Two diagnostic tests were performed with the opposed flow set-up to test this theory. The opposed flow set-up was used with N_2 being blown from the top jet toward the plasma to keep any ambient air from interfering with the experiments (although this effect was not expected in the reverse injection set-up either). First, the ability of the NO/NO_x analyzer to read ammonia was tested by running the ammonia and argon plasma gases through the test set-up without igniting the plasma. This test indicated that a small amount of ammonia is read by the NO channel of the analyzer (20 ppm at 0.16 lpm ammonia flow rate). However, the NO_x channel responds readily to ammonia, reading better than 2000 ppm at the same conditions, and this is consistent with the literature on interference effects in NO/NO_x analyzers.[16] Since the response of the NO channel to ammonia is small, and since it is expected that the majority of the ammonia is destroyed by passing it through the plasma, other species likely are causing additional interference problems.

A diagnostic test without the injection of NO toward the plasma chamber was conducted with the plasma running with ammonia addition. Figure 4.13 shows the NO and NO_x concentration readings as a function of plasma power for ammonia flow rates of 0.1 lpm and 0.2 lpm. Recall that the NO_x concentration readings include the concentration of NO, and that there is no source of oxygen in this experiment. As shown, the concentration of NO as read by the analyzer is significant, and the NO reading decreases as plasma power is decreased and as ammonia flow rate is increased. This is the same trend as observed in the reverse injection experiments; however, the amount of NO "produced" is not enough to negate the reductions found in the experiments, and so the trends reported are valid. It is acknowledged that the interference effect is confounded with the reduction effect. Finally, it is worthy of note that since the NO_x readings are well below those observed without plasma ignition, it is clear that most of the ammonia is being destroyed by the plasma. It is unknown, however, exactly what species are being formed.

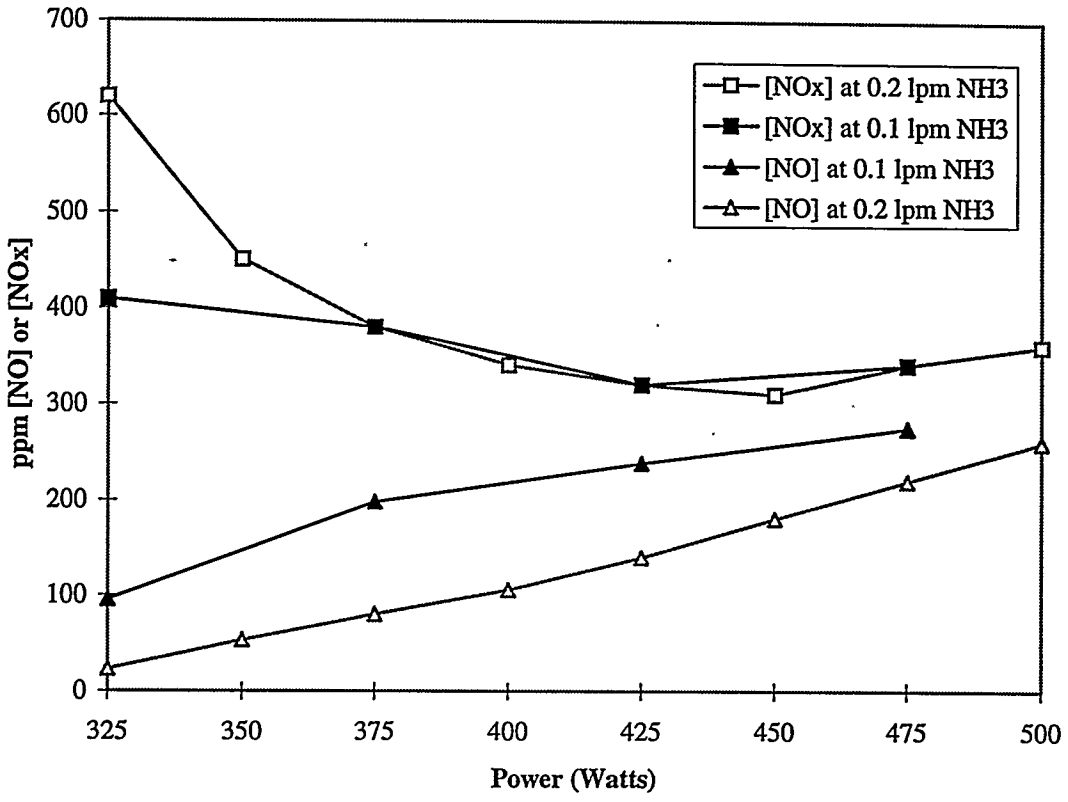

Figure 4.13: Diagnostic test showing apparent NO production in an oxygen-free environment.

Since the exact species formed by the ammonia-doped plasma are unknown, it is impossible to determine what exactly is causing the erroneous NO readings. A review of available NO/NO_x analyzer diagnostic literature failed to find reports of interference of NH_i species with measurements, except for NH_3 as already noted. However, the literature did provide precedence of interference that suggest at least one mechanism for the erroneous readings. The NO channel measures NO by reacting it with ozone (O_3) to form an excited NO_2 molecule; the subsequent chemiluminescence of that molecule as it reverts to its ground state is monitored and is proportional to the original NO concentration. A few species are reported to react with ozone and emit light at wavelengths that the NO_x analyzer recognizes as NO. Grosjean and Harrison[17] found a small positive response on the NO channel of their analyzer to several organosulfur compounds. The maximum response reported was less than 0.6% of the species concentrations, which were generally tested at less than 1 ppm. However, for the amount of ammonia passing through the plasma, a 0.6% erroneous reading could translate into significant NO interference readings. Tidona et al.[18] tested the interference of CO on the NO channel of a chemiluminescent

analyzer at higher concentrations. They found that the analyzer response to CO varied according to an expression involving the cube of the CO concentration. At 50% CO, the analyzer read approximately 800 ppm NO.

Thus, there is significant precedence for NO interference in chemiluminescent instruments, although the exact mechanism for the interference seen in the reverse injection experiments is a matter of conjecture. The diagnostic tests indicate that the interference effect is not sufficient to invalidate the parametric trends observed during testing of the plasma deNO$_x$ process. The data from the demonstration experiments are less affected by the interference phenomenon due to the larger scale of the experimental set-up. That is, the ratio of the amount of plasma gases to the combustion flue gases is sufficient to dilute the effect, and additional reactions may occur to destroy the interfering species in the larger system.

Conclusions

The reverse injection experiment successfully demonstrated several parametric effects on plasma deNO$_x$ performance. NO reduction improved with decreasing plasma power, increasing ammonia flow rate, and increasing NO-stream temperature. Both decreasing the plasma power and increasing the ammonia flow rate served to decrease the temperature of the plasma, as measured at a stationary location above the plasma device. The initial addition of ammonia to the plasma dropped its temperature considerably, while a second temperature drop was seen after the ammonia was increased somewhat. This temperature drop is suspected to alter the species produced by the ammonia-doped plasma, and this effect will be tested with kinetic modeling in Chapter 5.

It was also shown that the plasma deNO$_x$ process is effective at NO-stream temperatures significantly outside of the SNCR temperature window. The best performance of the reverse injection experiment showed 67% NO reduction with a plasma operating at 300 Watts and an NO-stream temperature of approximately 900 K. Increasing the stream temperature did not lead to additional NO reduction. Also, significant NO reduction occurred at temperatures below 900 K, and the limit of the process at some plasma powers was left undetermined due to stability problems with the plasma. The temperature limit of the process will also be explored numerically in Chapter 5.

Chapter 5: Assessment of Plasma DeNO$_x$ Modeling Feasibility

Chemical Kinetics Modeling

A plasma is a complex collection of charged and neutral gases that exhibit collective behavior, and as such it is a difficult system to model. For the preliminary analysis of general trends associated with temperature, this section will use a simple chemical kinetics model to look at the factors that affect radical generation and NO reduction. Following this analysis, a short review of current plasma modeling efforts will be presented, particularly with regard to their potential application to the design of the plasma deNO$_x$ process.

The chemical kinetics model used in the present analysis is a modified version of CHEMK,[19,20] and the reaction mechanisms are adopted from work by Boyle et al.[21] Two reaction mechanisms were considered. The first consisted of 32 reactions involving only hydrogen- and nitrogen-containing species and was used to investigate the effect of temperature and time on NH_3 dissociation. The second reaction mechanism consisted of 152 reactions involving hydrogen-, nitrogen-, and oxygen-containing species. This mechanism was used to investigate the effect of time and temperature on NO reduction.

To investigate NH_3 dissociation, a mixture of 1% NH_3 in a non-reacting gas was simulated at several temperatures to study the evolution of NH_i radicals over time. The temperature in this experiment may be considered an "effective plasma temperature" while the time would correspond to the residence time of the argon/ammonia mix in the high temperature plasma region. Figure 5.1 shows results similar to Boyle et al. indicating that higher temperatures lead to higher concentrations of radicals, but only for shorter residence times. Of course, residence time and temperature are coupled in plasma operation; however, for the current plasma geometry and flow conditions, a residence time on the order of milliseconds is expected. On that time scale, Figure 5.1 shows that a lower temperature plasma would lead to higher radical concentrations than the higher temperature plasma. This may be an explanation as to why lower power (and therefore lower temperature) plasma deNO$_x$ processes perform better.

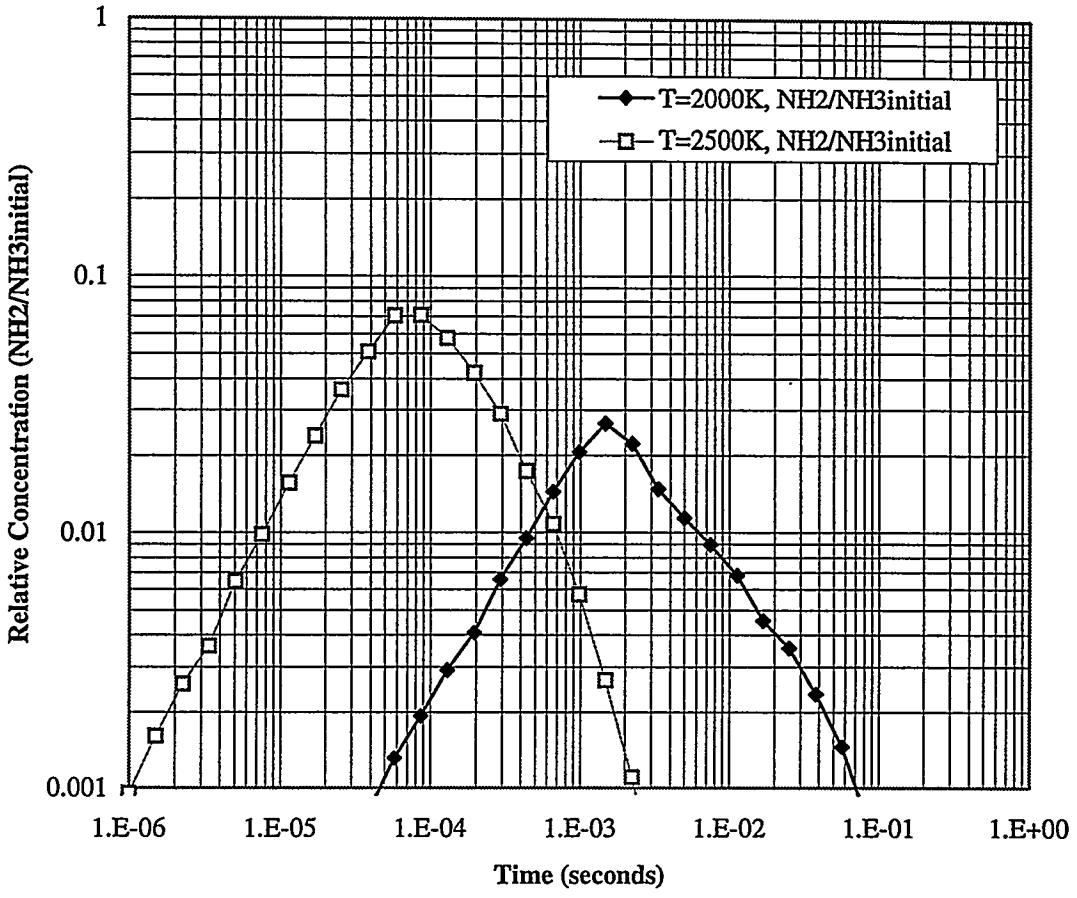

Figure 5.1: Relative NH_2 radical concentrations produced over time at an effective plasma temperature of 2000 K and at 2500 K.

Similarly, Figures 5.2 and 5.3 show the concentrations of NH_i species relative to the initial NH_3 concentration as a function of effective plasma temperature at two different residence times. Figure 5.2 corresponds to a residence time of 1 millisecond while Figure 5.3 corresponds to a residence time of 5 milliseconds. As shown, the concentrations of radicals produced are very small when only thermal dissociation is considered. Also, the NH_2 concentration peaks at a different temperature for each residence time. This may be relevant to choosing a plasma gas flow rate given a plasma power, which would be analogous to setting the residence time for a given temperature.

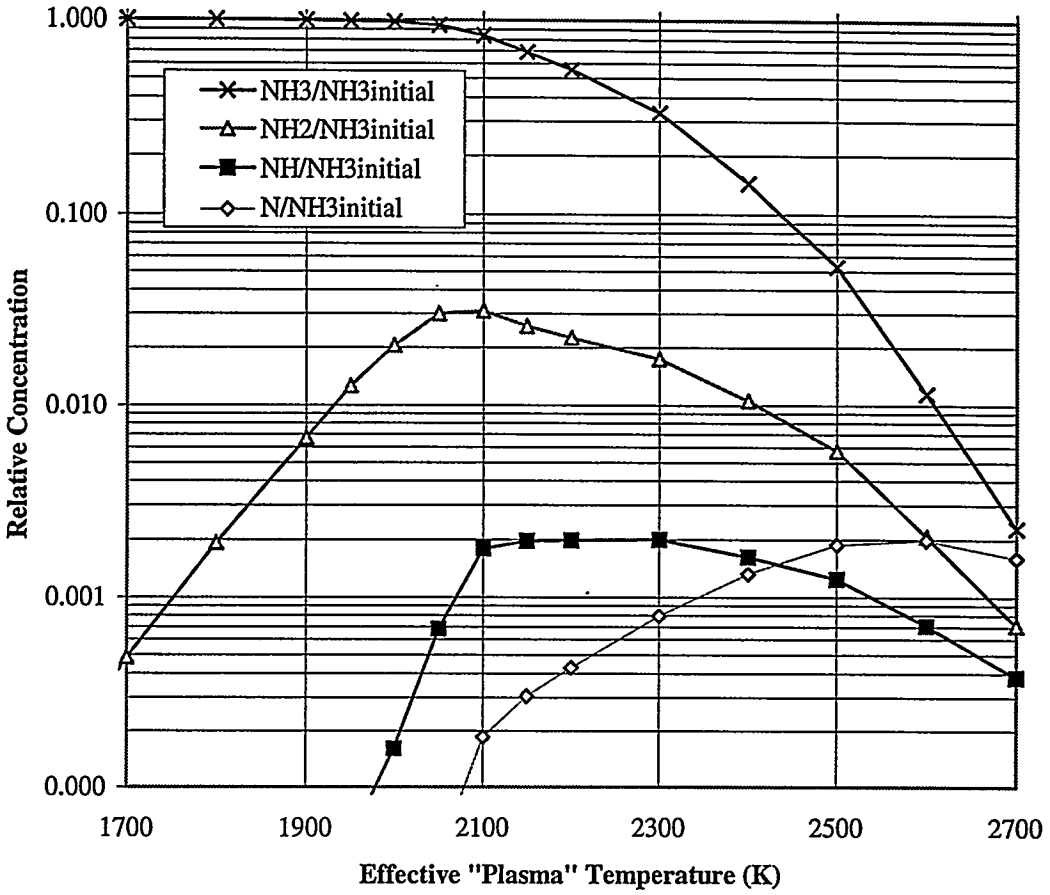

Figure 5.2: Relative concentrations of NH_i species as a function of effective plasma temperature for a 1 millisecond residence time.

The second phase of the CHEMK analysis took the species produced in the NH_3 dissociation step and simulated NO reduction at various reaction temperatures. Figure 5.4 shows typical results using initial species conditions generated by an effective plasma temperature of 2100 Kelvin and a residence time of 1 millisecond. The initial NO concentration was set to 600 ppm; thus, the overall NH_3/NO_x ratio in this simulation is approximately 17. While the reverse injection experiment reaction time was estimated to be less than 1 second, the simulation was carried out to 5 seconds to capture the effect of longer reaction times. As shown, the reaction temperature had little significant impact on the first phase of NO reduction, which was completed by 0.1 milliseconds. This reduction step is attributable to the presence of the NH_2 radicals produced by the plasma. However, because very few radicals were produced in the NH_3 dissociation step at the conditions stated, complete NO reduction is not achieved, even at such a high NH_3/NO_x ratio. This would explain the similar effect seen in the reverse injection experiment. The second reduction step in Figure 5.4 is attributable to the further dissociation of

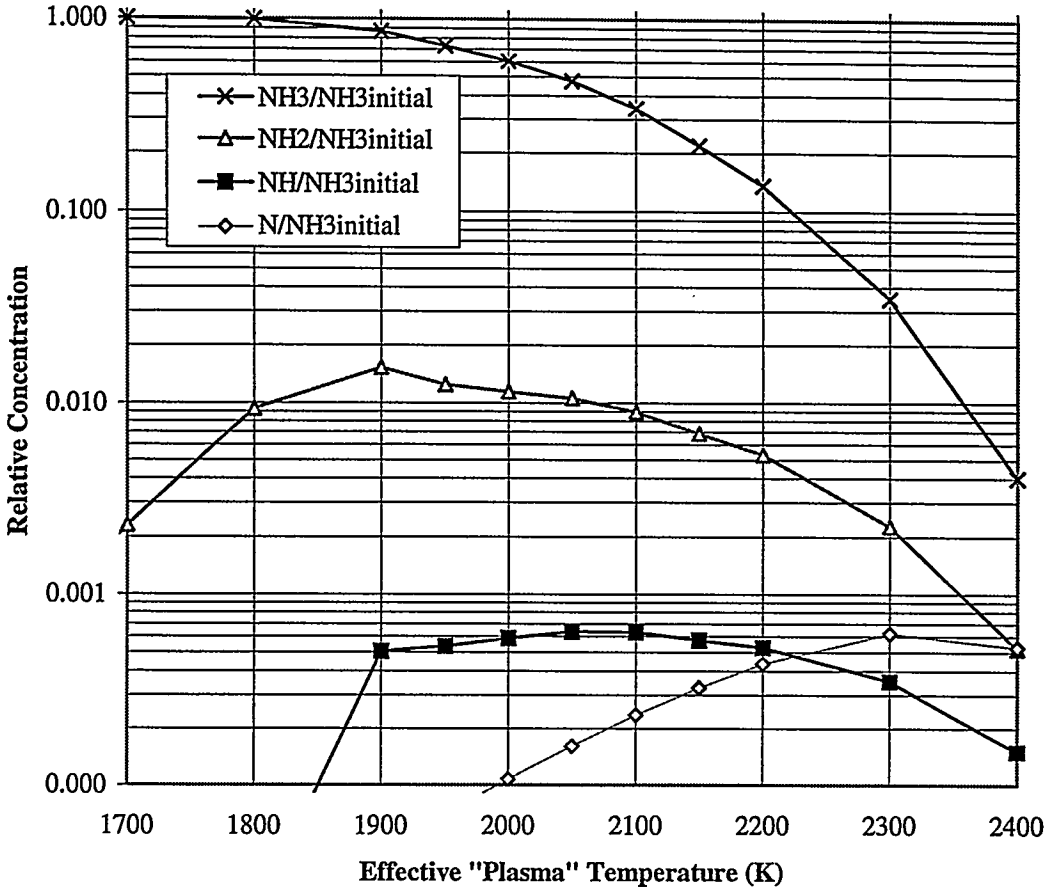

Figure 5.3: Relative concentrations of NH_i species as a function of effective plasma temperature for a 5 millisecond residence time.

NH_3 into NH_2 and subsequent reaction with NO. The inefficiency of this process at lower temperatures is compensated for by the high NH_3/NO_x ratio. A colder reaction temperature requires a longer time for NH_3 dissociation. Since the reverse injection experiment reaction time was less than 1 second and at lower temperatures, these CHEMK results would indicate that the reductions seen in that experiment were due to plasma-produced radicals and not to longer term NH_3 dissociation.

Numerical Modeling of Plasmas

While the chemical kinetics modeling is useful to evaluate trends and qualitative effects of different parameters, a detailed model of the IC plasma as used in the plasma deNO_x process would be useful in the eventual design and optimization of the process. The inductively coupled plasma was developed in the early 1960's and has since been used in a variety of applications including chemical analysis and synthesis, spheroidization, and extractive metallurgy.[22] As these

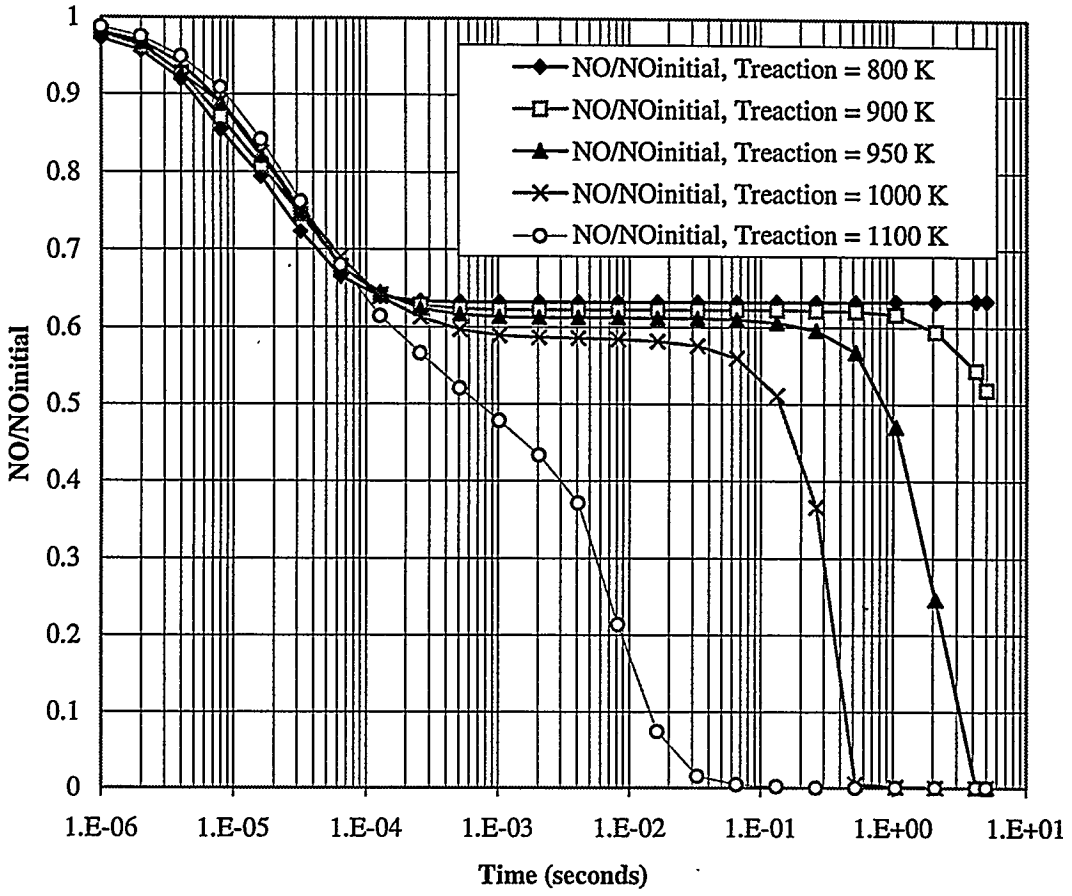

Figure 5.4: NO/NOinitial vs. time resulting from the dissociation of 1% NH_3 at 2100 K for 1 millisecond.

processes have been developed, modeling capabilities to describe the temperature, flow, and concentration fields have been developed as well. This section is meant to describe current plasma modeling capabilities and to highlight their relevance to the plasma deNO_x process development.

The first IC plasma models were one-dimensional mathematical models that focused on describing the temperature fields across the center of a plasma discharge by use of an energy balance approach.[23] These one-dimensional models, however, do not describe the temperature field outside of the induction zone, and they do not give information regarding the flow field in the torch. Two-dimensional models do provide this information, and are the current state-of-the-art in plasma modeling.

Two-dimensional modeling of the IC plasma involves the use of continuity, momentum, energy, and mass transfer equations along with electromagnetic field equations. Reference 22 provides an example of such a model in an analysis of the effect of different process parameters

on flow and temperature fields, and a summary of part of this work (as applicable to the plasma $deNO_x$ process) is reported here. Figure 5.5 is reproduced from Reference 22 to show typical results of plasma modeling efforts. The modeled plasma is operating at 1000 Watts, or roughly three times that used in the plasma $deNO_x$ experiments, but the frequency used is similar, and there is no central gas flow. As shown in the middle figure, the temperature of such a plasma can reach over 10,000 Kelvin in its center, with very high temperature gradients in the radial direction. It is also worthy to note in the first figure that there is an inward radial flow, which in the plasma $deNO_x$ process would indicate that some of the ammonia may be delivered to the high temperature region in the center of the plasma as well as through the cooler outer wall region (at least at higher powers).

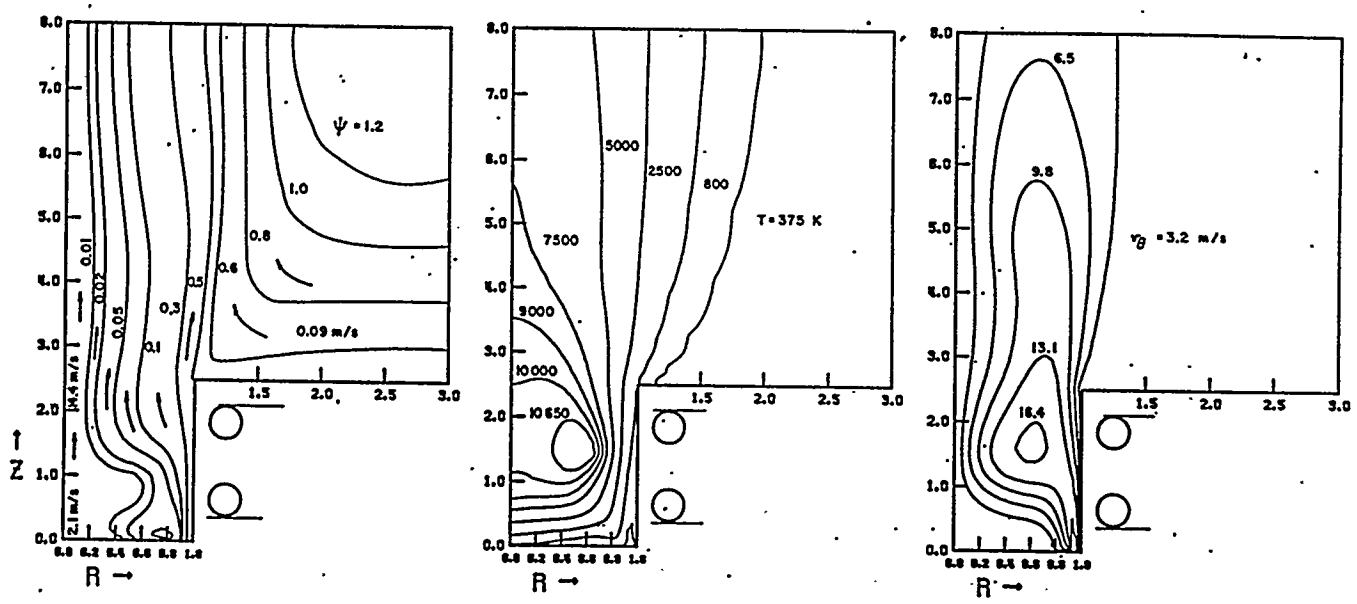

Figure 5.5: Reproduced from Boumans, 1987. Figure shows results of modeling of IC plasma operating at 26.3 MHz, 1000 Watts. Argon flow rates are 9 lpm, 1 lpm, and 0 lpm, for the outer, inner, and central flows, respectively. From left to right, streamlines, temperature, and swirl velocity are shown.

The calculation of concentration fields would be extremely useful in modeling the plasma $deNO_x$ process. Unfortunately, IC plasma modeling efforts are mainly concerned with concentration fields in the presence of a central gas stream used for spectroscopy or chemical synthesis work, and this stream is not used in the current plasma $deNO_x$ process. In modeling the concentration fields in Reference 22, the presence of a tracer in the central gas stream was assumed. The tracer had no effect on the thermodynamic or transport properties of the modeled

plasma, but it did diffuse throughout the plasma. It may be possible to use this same technique in modeling the plasma deNO$_x$ process, such that the concentration of ammonia in plasma discharge regions at different temperatures could be determined. The effect of temperature on ammonia dissociation could then be used to roughly predict radical generation.

More recent plasma modeling efforts have included a two-temperature model in which there is a significant difference in the electron and heavy particle temperatures in the plasma stream.[24] This and other models are concerned with the state of equilibrium (or lack thereof) in the plasma, and is beyond the scope of this report. However, the two temperature model is mentioned because the difference between the electron and atom/ion temperatures predicted can be of the order of 2000 K in at least one application,[25] and this would have a significant effect on radical generation. In addition, the two-temperature model predicts temperatures significantly below those predicted by other models that assume local thermodynamic equilibrium (such as in Reference 22), which would also affect radical generation predictions.

Finally, the addition of diluent gases to the outer plasma stream has some use in some laboratory work, and these types of plasmas are just beginning to be modeled in earnest. Gordon and Kruger[26] offer an example of this work. They show that the addition of less than 1% of hydrogen or nitrogen to the outer argon flow in the ICP drives the plasma out of even partial local thermodynamic equilibrium by "quenching" argon emission by reaction with the diluent. In addition, Gordon and Kruger mention that the depopulation of argon's excited states reduces the plasma's radiative loss rate. This effect may be significant in designing the plasma deNO$_x$ system for efficient radical generation.

Conclusions

The chemical kinetics modeling of NH_3 dissociation and subsequent NO reduction demonstrated several qualitative trends that are useful to the design and optimization of the plasma system for the plasma deNO$_x$ process. The importance of effective plasma temperature and residence time on radical generation was shown. Without efficient radical generation, the process relies on the dissociation of ammonia, which is a much slower process and prone to ammonia slip. Optimizing the efficiency of radical generation will be critical in the design of plasma deNO$_x$ for commercial application.

This chapter has also considered the applicability of current plasma modeling capabilities to the design of the plasma deNO$_x$ process. Several two-dimensional models predict temperature and flow fields in an inductively coupled plasma. These models differ in the equilibrium assumptions used to describe the state of the plasma, and it is likely that a non-LTE model is necessary to simulate the plasma with significant ammonia addition. Current modeling capability to predict the concentration of radicals that would be emitted from the plasma deNO$_x$ process appears to be limited to tracing the diffusion of a species in the plasma flow field, without accounting for the effect on the plasma characteristics or plasma-tracer interactions. However, even without accounting for plasma-tracer interactions, calculating the temperature-time history of ammonia as it diffuses through the plasma is an important future step to accurately predicting radical generation and optimizing the plasma deNO$_x$ process. That is, once the concentration of species as diffused throughout the plasma were known, the temperature fields could be used to approximate NH_i production by thermal dissociation, and the effects of plasma parameters such as frequency, flow rates, and power on radical generation could be studied numerically.

Chapter 6: Summary and Recommendations

This report has presented several experiments designed to explore the mechanisms that lead to good performance of the plasma deNO$_x$ process for NO$_x$ control from stationary combustion sources. The hot ammonia injection experiment described in Chapter 2 demonstrated that the benefit of treating the ammonia with the plasma for radical generation is more than just the benefit of the bulk heating of the reagent stream. The "plasma effect" accounted for an additional 15-35% absolute NO$_x$ reduction over the hot NH$_3$ injection performance at 0-25% excess air. The benefit of using the plasma for radical generation increased as the excess air was increased and as the combustor flue stream temperature was decreased. It was also shown that hot ammonia injection processes provide only modest improvement to cold SNCR processes at typical NH$_3$/NO$_x$ ratios and combustor operating conditions.

The study of the plasma deNO$_x$ system at the local level proved difficult for a number of reasons. One of the findings of practical importance in designing a plasma deNO$_x$ system was the production of NO by the plasma when operating in an air environment. This production can be avoided by maintaining an oxygen-free zone in the vicinity of the plasma. A second difficulty in studying the plasma was the apparent interference of other species on the NO channel of the NO/NO$_x$ analyzer. This problem was quantified, and it was found that the interference decreased with plasma power. The magnitude of the interference was not sufficient to mask the desired parametric studies. The interference and NO "production" effects were probably not seen in the demonstration experiments because the volume of the combustion flue gases would have diluted the effects.

The reverse injection experiment demonstrated the effect of several key parameters on plasma deNO$_x$ performance. First, it was verified that, for identical test conditions, use of a lower power plasma led to better NO$_x$ reduction in the range of 250-400 Watts. It was also found that higher ammonia flow rates led to better NO$_x$ reduction; however, rather than being a direct result of the increase in the NH$_3$/NO$_x$ ratio, it was suggested that the addition of ammonia to the plasma also led to a decrease in plasma temperature, which leads to better radical production in a manner analogous to power reduction. The drop in plasma temperature, as measured at a single

location above the source, was documented. The reverse injection experiment also demonstrated that the lower limit of the temperature window for the plasma deNO$_x$ process is significantly below that required for SNCR. Good NO$_x$ reduction was achieved at temperatures below 900 Kelvin. Lower operating temperatures may be effective when radical production by the plasma is optimized.

The optimization of radical generation is critical to the efficiency of the plasma deNO$_x$ process. Simple chemical kinetics modeling demonstrated that the production of NH_2 radicals in the plasma is dependent on both the effective plasma temperature and the residence time of the reagent at that temperature. At higher temperatures, the relative concentrations of radicals produced is higher, but only if the residence time of the ammonia in the high temperature zone of the plasma is very short. For longer residence times, the operating temperature of the plasma must be cooler to optimize radical production. It was also shown that the magnitude of the relative radical concentration achieved in the simple kinetic modeling was very small, only a few percent in the example shown. Kinetic modeling showed that while these radicals react very quickly with NO, the generation of more radicals by the breakdown of excess ammonia was temperature and time dependent. The temperature and the time scale of the reverse injection experiments suggest that the NO reduction achieved was a result of the reaction of plasma-generated radicals alone. However, due to the longer reaction time allowed in the demonstration experiments, part of the achieved reduction may be attributable to thermal NH_3 dissociation. This is consistent with the hot NH_3 injection experimental results, in addition to the chemical kinetic modeling.

The long term optimization of the plasma deNO$_x$ process should concentrate on radical production in the design of the plasma device used. Current IC plasma modeling capabilities were reviewed to assess the feasibility of using mathematical models in this design process. It does not appear possible to accurately model the interaction of the ammonia with the plasma; however, it should be possible to track the diffusion of the reagent through the plasma discharge. Coupled with the modeling of the temperature field in the plasma and the chemical kinetic work described, this would be an important step toward accurately predicting radical generation in the plasma by tracing the temperature-time history of injected ammonia. It should be noted that the plasma with significant ammonia injection is likely to not be in local thermodynamic

equilibrium, which further complicates the modeling task. Because of the difficulties in modeling the plasma deNO$_x$ process, experimental work will be required to verify any results obtained.

The next round of experiments in the development of the plasma deNO$_x$ process should concentrate on the parameters of the IC plasma, as well as other plasma devices, that affect performance. For example, it is known that higher frequency plasmas operate at lower temperatures for the same power and flow conditions (see, for example, Mostaghimi and Boulos, 1990). In addition, the DC plasma used by Boyle et al. in the other plasma deNO$_x$ demonstration experiment deserves further study.

References

1. Possiel, N. C., Editor. U.S. Environmental Protection Agency. "Regional Ozone Modeling for Northeast Transport (ROMNET)", Office of Air Quality Planning and Standards, Technical Support Division, Research Triangle Park, NC, 1991 (EPA-450/4-91-002a).

2. Bachman, John. "Atmospheric Nitrogen Oxides: A Bridesmaid Revisited", presented at the American Chemical Society Symposium on "Quantitative Ranking of Environmental Problems According to Risk", August 28, 1991.

3. Lyon, R.K. "Method for the Reduction of the Concentration of NO in Combustion Effluents Using Ammonia," U.S. Patent 3,900,554 assigned to Exxon Research and Engineering Company, 1975.

4. Salimian, S. and Hanson, R.K. "A Kinetic Study of NO Removal from Combustion Gases by Injection of Nhi-Containing Compounds," Combustion Science and Technology, 1980, 23:225.

5. U.S. EPA. "Summary of NOx Control Technologies and their Availability and Extent of Application," Office of Air Quality Planning and Standards, Research Triangle Park, NC, 1992 (EPA-450/3-92-004).

6. U.S. EPA. "Alternative Control Techniques Document – NOx Emissions from Utility Boilers," Office of Air Quality Planning and Standards, Research Triangle Park, NC, March 1994 (EPA-453/R-94-023).

7. Zhou, Q., Yao, S.C., Russell, A., and Boyle, J. "Flue Gas NOx Reduction Using Ammonia Radical Injection," Journal of the Air and Waste Management Association, 1992, 42:1193.

8. Boyle, J., Russell, A., Yao, S.C., Zhou, Q. Ekmann, J., Fu, Y., and Mathur, M. "Reduction of Nitrogen Oxides from Post-Combustion Gases Utilizing Molecular Radical Species," Fuel, 1993, 72:1419.

9. Zhou, Q., 1991. "The Effect of Plasma Injection on NOx Emissions for Pulverized Coal Combustors," Ph.D. Thesis, Carnegie Mellon University.

10. Lyon, R.K. "Thermal DeNOx," Environmental Science & Technology, 1987, 21:231.

11. Offen, G.R., Eskinazi, D., McElroy, M.W., and Maulbetsch, J.S., "Stationary Combustion NOx Control," JAPCA, 1987, 37:864.

12. Burns and Roe Company, "Preliminary Economic Assessment [of] PETC Radical Injection Process for NOx/SOx Control," report prepared for Pittsburgh Energy Technology Center, U.S. Department of Energy, 1992.

13. Potter, A.E. and Butler, J.N., 1959. "A Novel Combustion Measurement Based on the Extinguishment of Diffusion Flames," ARS Journal, 29: 54-56.

14. Hahn, W.A., Wendt, J.O.L., and Tyson, T.J., 1981. "Analysis of the Flat Laminar Opposed Jet Diffusion Flame with Finite Rate Detailed Chemical Kinetics," Combustion Science and Technology, 27: 1-17.

15. Miller, E. and McMillion, L.G., 1992. "The Suppression of Opposed-Jet Methane-Air Flames by Methyl Bromide," Combustion and Flame, 89: 37-44.

16. Klapheck, K. and Winkler, P., 1985. "Technical Note: Sensitivity Loss of a NOx-Chemiluminescent Analyzer Due to Deposition Formation," Atmospheric Environment, 19:9, 1545-1548.

17. Grosjean, D. and Harrison, J., 1985. "Notes: Response of Chemiluminescence NOx Analyzers and Ultraviolet Ozone Analyzers to Organic Air Pollutants," Environmental Science and Technology, 19:9, 862.

18. Tidona, R.J., Nizami, A.A., and Cernansky, N.P., 1988. "Reducing Interference Effects in the Chemiluminescent Measurement of Nitric Oxides from Combustion Systems," JAPCA, 38: 806-811.

19. McRae, G.J., 1983. "A Program for the Numerical Solution of Chemical Kinetics Problems," Environmental Quality Laboratory 206-40, California Institute of Technology, Pasadena, CA.

20. Whitten, G.Z. and Hogo, H., 1980. "Modeling of Simulated Photochemical Smog with Kinetic Mechanisms Volume 2, CHEMK: A Computer Modeling Scheme for Chemical Kinetics," U.S. Environmental Protection Agency Report No. EPA-600/3-80-026b, Research Triangle Park, North Carolina.

21. Boyle, J., Russell, A.G., Yao, S.C., Zhou, Q., Ekmann, J., Fu, Y., and Mathur, M., 1992. "Reduction of Nitrogen Oxides from Post-Combustion Flue Gases Utilizing Molecular Radical Species," Fuel.

22. Boumans, P.W.J.M., Ed., 1987. Inductively Coupled Plasma Emission Spectroscopy, Part 2: Applications and Fundamentals. John Wiley & Sons, New York, 1987.

23. See, for example, Freeman, M.P. and Chase, J.D., 1968. Journal of Applied Physics, 39: 180.

24. Mostaghimi, J., Proulx, P., and Boulos, M., 1987. "A Two-Temperature Model of the Inductvely Coupled RF Plasma," Journal of Applied Physics, 61(5): 1753.

25. Mostaghimi, J. and Boulos, M.I., 1990. "Effect of Frequency on Local Thermodynamic Equilibrium Conditions in an Inductively Coupled Argon Plasma at Atmospheric Pressure," Journal of Applied Physics, 68(6): 2643.

26. Gordon, M.H. and Kruger, C.H., 1993. "Non-Equilibrium Effects of Diluent Addition in a Recombining Argon Plasma," Physics of Fluids B, 5(3): 1014.